Progress in Polymer Science xxx (2015) xxx–xxx

Contents lists available at ScienceDirect

Progress in Polymer Science

journal homepage: www.elsevier.com/locate/ppolysci

Directed self-assembly of block copolymers by chemical or topographical guiding patterns: Optimizing molecular architecture, thin-film properties, and kinetics

Weihua Li[a,b,*], Marcus Müller[a,**]

[a] Institute for Theoretical Physics, Georg-August University, 37077 Göttingen, Germany
[b] State Key Laboratory of Molecular Engineering of Polymers, Department of Macromolecular Science, Fudan University, Shanghai 200433, China

ARTICLE INFO

Article history:
Received 21 January 2015
Accepted 26 October 2015
Available online xxx

Keywords:
Block copolymer
Directed self-assembly (DSA)
Chemoepitaxy
Graphoepitaxy
Thin film

ABSTRACT

Patterning strategies based on directed self-assembly (DSA) of block copolymers, as one of the most appealing next-generation lithography techniques, have attracted abiding interest. DSA aims at fabricating defect-free geometrically simple patterns on large scales or irregular device-oriented structures. Successful application of DSA requires to control and optimize multiple process parameters related to the bulk morphology of the block copolymer, its interaction with the chemical or topographical guiding pattern, and the kinetics of structure formation. Most studies have focused on validating DSA patterning techniques using PS-*b*-PMMA block copolymers as a prototypical material. As the development of DSA techniques advances, recent efforts have been devoted to extending the materials selection in order to fabricate more complex geometric patterns or patterns with smaller characteristic dimensions. How to select appropriate polymer materials in a vast parameter space is a critical but also challenging step. In this review, we discuss recent progress in the research of DSA of block copolymers focusing on three aspects: (i) screening the block copolymer materials, (ii) controlling the film properties, and (iii) tailoring the phase separation kinetics.

© 2015 Elsevier Ltd. All rights reserved.

Contents

1. Introduction 00
2. Materials selection: Screening molecular architectures 00
   2.1. AB diblock and ABA triblock copolymers 00
   2.2. Multiblock copolymers 00
   2.3. Blending and supramolecular polymer materials 00
3. Control film properties 00
4. Process-directed self-assembly: tailoring the kinetics of structure formation 00

* Corresponding author at: Georg-August University, Institute for Theoretical Physics, 37077 Gottingen, Germany.
** Corresponding author.
E-mail addresses: weihuali@fudan.edu.cn (W. Li), mmueller@theorie.physik.uni-goettingen.de (M. Müller).

http://dx.doi.org/10.1016/j.progpolymsci.2015.10.008
0079-6700/© 2015 Elsevier Ltd. All rights reserved.

Please cite this article in press as: Li W, Müller M. Directed self-assembly of block copolymers by chemical or topographical guiding patterns: Optimizing molecular architecture, thin-film properties, and kinetics. Prog Polym Sci (2015), http://dx.doi.org/10.1016/j.progpolymsci.2015.10.008

4.1. Surface-directed spinodal structure formation 00
4.2. Nucleation induced defect-free domain patterns 00
5. Perspectives 00
Acknowledgments 00
References 00

1. Introduction

Directed self-assembly (DSA) of block copolymers has attracted continuously increasing interest during the past twenty years because it combines the advantages of the traditional lithography and the self-assembly ability of spontaneously forming sub-30 nm nanostructures [1–4]. Therefore it is currently regarded as one of the most appealing next-generation lithography techniques [5–18]. Since a number of excellent, recent reviews have discussed different aspects of DSA [5–11,19], we only consider the structure formation of block copolymer materials in thin films that is steered by short-ranged chemical or topographical guiding patterns on the substrate. Specifically, we focus on three, important aspects of DSA: screening copolymer materials, optimizing film properties, and tailoring the self-assembly kinetics.

The self-assembly of block copolymers in bulk or in thin films supported by a uniform substrate rarely leads to the desired, perfectly ordered structures. Although such structures represent the thermodynamic equilibrium, the system is readily trapped kinetically into one of a multitude of metastable defective morphologies of the free-energy landscape [16,19–23]. Usually these metastable morphologies are long-lived relative to experimentally accessible time. Consequently, various external fields, including long-range fields (electric, magnetic or shear) and short-range fields (i.e., topographic or chemical surface patterns), have been devised to guide the self-assembly of block copolymers to form desired nanostructures. Long-range fields, e.g. shear [10,24–33] and electric fields [34–44], aim at controlling the overall orientation of structures on large length scales. It remains, however, a challenge to fulfill the stringent requirements on defect densities and precise registration with external device components required by semiconductor industries. Alternatively, short-range guiding fields, i.e. chemical (chemoepitaxy) [14,17,45,46] or topographical (graphoepitaxy) [16,20,47–49] guiding patterns on the substrate, have been demonstrated to achieve structures satisfying the demands of semiconductor applications. Moreover, DSA employing chemoepitaxial or graphoepitaxial techniques can be applied to fabricate not only large-scale, defect-free, geometrically simple patterns but also device-oriented, irregular or aperiodic structures that differ from the bulk phases of block copolymers, e.g. structures that resemble integrated circuits [15,18,49–56].

The fundamental idea of DSA is to encode the short-scale part of pattern information into the molecular architecture of block copolymers; in turn, the lithographically prepared guiding pattern only directs the orientation on larger scales and controls the registration of block copolymer structures with external boundaries. The most extensively studied block copolymer in DSA is the simplest AB diblock copolymer, which is composed of two chemically different, linear, flexible chain molecules that are joined at their ends by covalent bonds. The phase behavior of AB diblock copolymer is dictated by two parameters: the volume fraction f of A block and the degree of incompatibility χN between the two blocks, where χ denotes the Flory–Huggins interaction parameter and N is the total number of segments. By varying f from symmetric to asymmetric, AB diblock copolymers can self-assemble into a sequence of ordered phases, encompassing lamellar, gyroid or *Fddd* network, hexagonally-arranged cylindrical, and body-centered-cubic (bcc) spherical phases in the bulk [57–59]. Among these phases, the lamellar and cylindrical phases have been frequently and successfully utilized to fabricate large-scale geometrically simple stripe patterns (lines and spaces) [14,17,45,46] and hexagonal cylinder patterns (a triangular lattice of standing cylinders) [16,17,60], respectively. Intuitively, the guiding patterns are designed to have similar symmetries and commensurate periods as the domain structures of block copolymers. In particular, the guiding pattern can have an integer multiple of periods to the domain period of the bulk phase in order to enable a density multiplication [16,17,45,60–62], which is useful to reduce the manufacturing cost of the guiding pattern. In contrast, for the alternative task to fabricate device-oriented irregular structures, the design of guiding patterns becomes much more challenging. Besides trial-and-error approaches, computer simulations have been employed to optimize the guiding patterns by solving the self-assembling structures on various guiding patterns with appropriate theoretical models, such as the self-consistent field theory (SCFT) [54] and the time-dependent Ginzburg–Landau theory (TDGL) of the Ohta–Kawasaki free energy functional [55]. Compared with the first task, most of the research aiming at fabricating irregular structures has been carried out only with AB diblock copolymers and mixtures with their respective homopolymers, and hence is still in the infancy stage. Additional details can be found in recent reviews [5–11,19].

Intrinsically, cylinder-forming AB diblock copolymers self-assemble so that the cylinders are arranged on a triangular lattice. In semiconductor applications, however, a square arrangement of cylinders would be more convenient [63,64]. Even imposing a strong external field, e.g. laterally square confinement, it remains difficult to achieve a square pattern with cylinder-forming AB diblock copolymer [64,65]. An promising approach consists in replacing linear AB block copolymers with other copolymer architectures that form an ordered phase of tetragonal symmetry, such as symmetric ABC linear triblock copolymers whose equilibrium phase diagram comprises a phase of alternatively arranged A and C cylinders on a tetragonal lattice [1,66,67]. Alternatively, supramolecular architectures (in conjunction with chemical guiding patterns) can

Please cite this article in press as: Li W, Müller M. Directed self-assembly of block copolymers by chemical or topographical guiding patterns: Optimizing molecular architecture, thin-film properties, and kinetics. Prog Polym Sci (2015), http://dx.doi.org/10.1016/j.progpolymsci.2015.10.008

be employed to fabricate square tic-tac-toe structures with various dimensions [68]. These examples demonstrate that it is necessary to turn to more complex molecular architectures of block copolymers in order to enrich the structure types generated by DSA and thus to widen the applications of DSA.

The fast development of modern synthesis techniques enables the generation of a variety of complex (multi)block copolymers and hence opens opportunities for DSA to fabricate geometrically complex structures. At the same time, however, there is a big challenge for DSA to tailor the architecture of copolymer materials for specific targeted structures [4]. On one hand, one needs to explore the phase diagrams in the bulk for candidate block copolymers. SCFT has been developed as one of the most efficient methods for exploring phase diagrams of block copolymers [57,69–71]. However, the calculation capability strongly relies on the dimension of parameter space. For two component systems, e.g. AB or symmetric ABA block copolymers, there are only two parameters and an exhaustive exploration of parameter space is computationally affordable. When one more component is introduced, e.g. ABC triblock copolymer, the parameter space is enlarged to at least five dimensions, χ_{AB}, χ_{BC}, χ_{AC}, f_A and f_B, and thus a systematic exploration of the entire parameter space is a formidable task [59,67,72–74]. Importantly, the self-assembly of ABC linear [1,66,75–80] or star [81–84] triblock copolymers has been intensively studied by both experiment and theory, and as a consequence, a large number of intriguing nanostructures have been discovered including tetragonal A/C cylinders, A/C spheres alternatively arranged on a CsCl crystal lattice [67,72], supercylinders decorated by single/double/triple helices [73], and knitting patterns [74]. Moreover, recently Xie et al. have proposed a useful design principle for rationalizing the formation of sphere and cylinder phases in ABC multiblock terpolymers [85]. This new concept allowed them to fabricate desired nanostructures via the self-assembly of multiblock terpolymers by exploiting universal design principles to rationally encode structural information into the macromolecular architecture instead of exploring the entire parameter space. Incorporating these design principles into DSA promises to open avenues for fabricating complex periodic structures. The challenge consists in generalizing these design principles from bulk phases to geometrically confined systems, i.e. thin films, topographically structured substrates or contact holes, and chemically patterned surfaces.

In addition to the molecular architectures, the phase behavior of block copolymers can be modified by blending distinct polymers together. Addition of homopolymers into block copolymers not only tunes the domain sizes by swelling corresponding domains but also alters the equilibrium phase by modifying the effective volume fractions [86–90]. Moreover, homopolymers have been successfully employed to act as "defectants" (similar as surfactant stabilizing interfaces by reducing interfacial tension, "defectants" facilitate the stability of defects by releasing stress around defects) [68] in DSA to stabilize irregular structures. These additives segregate to non-bulk-like regions with high strain thereby lowering their free energy [15,19,50]. Blending block copolymers with various molecular weights, volume fractions, or molecular architectures, additionally provides a convenient way to fabricate new structures by altering e.g. the intrinsic interfacial curvature or characteristic length scale without the need of synthesizing new materials.

The phase behavior of block copolymers in thin films even overlying on a uniform substrate is very different from that in the bulk because the space symmetry of ordered phases is often broken by the presence of two surfaces. For example, the three-dimensional (3D) phases of AB diblock copolymers – bcc sphere and gyroid structures – cannot form in thin films when the thickness amounts to only a few domain periods; instead they usually transform into hexagonally close-packed sphere layers and perforated lamellae, respectively [91–93]. Only in a special case of two neutral surfaces, free-standing lamellae or cylinders, which inherit the characteristic feature of the bulk phases, can be formed. Otherwise, when one or two surfaces is preferential to one of components, the phase behavior becomes more complicated [94]. The confinement effect of thin film is able to induce order–order transitions (OOT). For instance, cylinder-forming diblock copolymer in thin films can self-assemble into parallel lamellar layers or perforated lamellae [93]. To control film properties, i.e. film thickness and surface interactions with each component, is a critical step for tailoring the formation of structures in DSA.

Besides the equilibrium thermodynamic properties, the kinetics of self-assembly plays a crucial role for the fabrication of desired structures by DSA. Usually, phase separation of block copolymers under typical processing conditions, solvent casting, thermal tempering or solvent annealing, initially proceeds via a spinodal mechanism. It has been proposed that most defects are created during this initial stage of structure formation because their excess free energy is too large for them to form by thermal fluctuations in a defect-free morphology [95,96]. To control the self-assembling kinetics via guiding patterns (e.g. via heterogeneous nucleation from a metastable disordered phase [97] or surface-directed spinodal structure formation [98]) offers opportunities to reduce the probability of defect formation and avoid grain formation. Moreover, temporal control of thermodynamic process parameters like pressure, temperature or solvent contents also opens avenues for tailoring the initial unstable state such that the spontaneous structure formation becomes trapped in a useful, novel metastable morphology instead of the equilibrium morphology [99].

In this review, we discuss strategies to fabricate tailored structures by directed self-assembly (DSA) of block copolymers. Since various directing techniques, distinguished by the preparation methods of guiding patterns, have recently been reviewed [10–12], we focus on additional key characteristics including (1) screening copolymer materials, (2) controlling thin-film properties, and (3) manipulating the kinetics of self-assembly. In order to achieve defect-free DSA of complex structures, these different aspects have to be optimized simultaneously. In Section 2, we discuss the distinct features of equilibrium self-assembled structures in various copolymer systems and highlight their relevance to applications in DSA. In Section 3, we focus on confinement effects, i.e. film thickness and surface interactions. In

Please cite this article in press as: Li W, Müller M. Directed self-assembly of block copolymers by chemical or topographical guiding patterns: Optimizing molecular architecture, thin-film properties, and kinetics. Prog Polym Sci (2015), http://dx.doi.org/10.1016/j.progpolymsci.2015.10.008

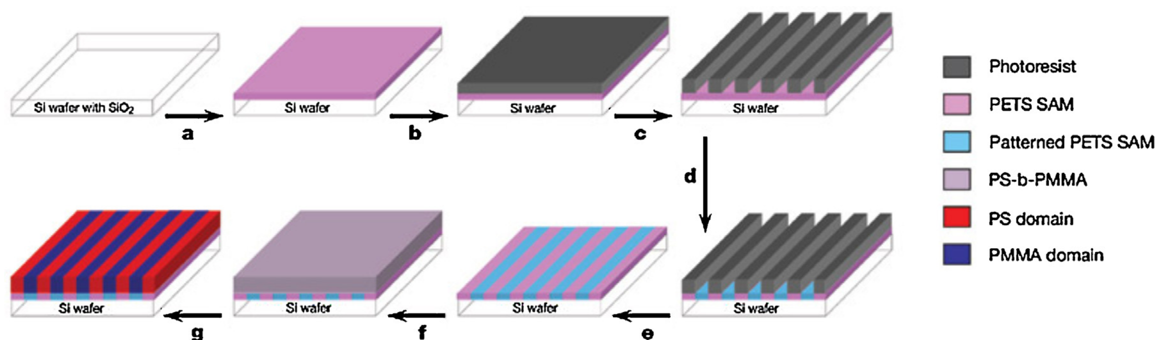

Fig. 1. Schematic representation of directed self-assembly of symmetric block copolymers on chemically patterned surfaces. (a) A self-assembled monolayer (SAM) of PETS is deposited on a silicon wafer. (b) Photoresist is spin-coated on the SAM-covered substrate, and (c) patterned by EUV-IL with alternating lines and spaces of period L_s. (d) The topographic pattern of the photoresist is converted to a chemical pattern on the SAM surface by irradiating the sample with soft X-rays in the presence of oxygen. (e) The photoresist is subsequently removed with repeated solvent washes. (f) A symmetric, lamella-forming PS-*b*-PMMA copolymer of period L_0 is spin-coated onto the patterned surface and (g) annealed, resulting in surface-directed block copolymer morphologies. Chemically modified regions of the surface are preferentially wetted by PMMA blocks, whereas unmodified regions do not exhibit a preference for any of the two blocks. Ref. [14], Copyright 2003. Reproduced with permission from the Nature Publishing Group.

Section 4, we present some aspects of the kinetics of self-assembly in the context of DSA. Section 5 concludes our review with a brief perspective.

2. Materials selection: Screening molecular architectures

2.1. AB diblock and ABA triblock copolymers

Both chemoepitaxy and graphoepitaxy techniques of DSA have been well developed and validated with both lamellar-forming and cylinder-forming AB diblock copolymers, especially with the standard model of diblock copolymer, polystyrene-*block*-polymethylmethacrylate (PS-*b*-PMMA) [14,15,46,50,100–103]. Fig. 1 illustrates the prototypical technique of chemoepitaxy for fabricating large-scale defect-free stripe patterns. It consists of two steps: fabrication of the chemical pattern on the supporting substrate using extreme ultraviolet interferometric lithography or e-beam lithography, and spin-coating lamella-forming PS-*b*-PMMA onto the chemically patterned substrate with a precisely controlled film thickness [14]. In the first step, the properties of the chemical pattern, i.e. the period, the width of the wetting stripe, and the contrast in interfacial energies between the blocks and the stripe domains of the chemical substrate pattern play a critical role for the directing quality of the chemical pattern and its ability to register the block copolymer stripes. Usually, the period of the pattern L_s and the width of the wetting stripe W are optimized to be $L_s \approx L_0$ and $W = 1/2L_0$, respectively, where L_0 is the domain period of the perpendicular lamellar morphology in a thin film on top of a uniform substrate [101]. It has been demonstrated that a larger contrast of interfacial interactions gives rise to a stronger directing ability [104]. In the second step, the film thickness is controlled by the speed of spin coating.

Using optimal values of $L_s = L_0$ and $W = 1/2L_0$, numerous experiments and simulations have demonstrated that chemically patterned substrates are capable to guide lamella-forming diblock copolymers to form defect-free stripes [14,101,104,105]. A small deviation of the two feature sizes from their optimal values, especially of the pattern period, can decrease the directing ability of guiding pattern, and results in the occurrence of defects that are detrimental to semiconductor applications. Kim et al. have investigated the influence of pattern period on the directing quality of chemical pattern to the self-assembly of symmetric PS-*b*-PMMA copolymers with $L_0 = 48$ nm (Fig. 2) [14]. With $L_s = 47.5$ nm, $L_s \cong L_0$, block copolymer lamellar domains are perfectly aligned and registered by the guiding pattern on the substrate (Fig. 2(b)). When L_s is decreased by 5%, i.e. $L_s = 45$ nm (Fig. 2(a)), the lamellar domains are compressed in order to replicate the guiding stripes. The registration degree is dictated by the competition between the free-energy penalty of domain compression and the benefit in interfacial energy with the guiding pattern. In Fig. 2(a), most part of the lamellar structure is registered but a certain concentration of dislocation pairs is present. In the space between pairs of dislocations, the domain stress is effectively released because of the reduced domain density.

In the opposite case, for $L_s > L_0$, the imperfection comes up in distinct mechanisms during the ordering of lamellar domains. When the incommensurability is small, e.g. $L_s = 50$ nm (see Fig. 2(c)), a defect-free and registered lamellar pattern is still obtained but the internal AB interfaces exhibit undulations along the stripe direction. These buckling effects are characteristic for stretched smectic phases [106]. As the deviation L_s/L_0 increases, e.g. $L_s = 52.5$ nm and 55 nm (cf. Fig. 2(d) and (e)), the lamellar domains no longer register perfectly with the guiding pattern. These experimental results on pure diblock copolymers conclude that the perfect epitaxial assembly on this chemically patterned surface occurs only if L_s is close to L_0.

Importantly, the directing quality of the chemical guiding pattern is also related to the contrast in interfacial energy of the patterned surface. Edwards et al. [104] implemented an approach to create the chemical patterns, which is proceeded via etching one layer of grafted PS-*r*-PMMA random copolymer brushes into equally spaced stripes intervened by oxidized (polar) surface area, which is strongly preferential to the PMMA block of the copolymer. The interfacial interaction of the brush-grafting stripe

Please cite this article in press as: Li W, Müller M. Directed self-assembly of block copolymers by chemical or topographical guiding patterns: Optimizing molecular architecture, thin-film properties, and kinetics. Prog Polym Sci (2015), http://dx.doi.org/10.1016/j.progpolymsci.2015.10.008

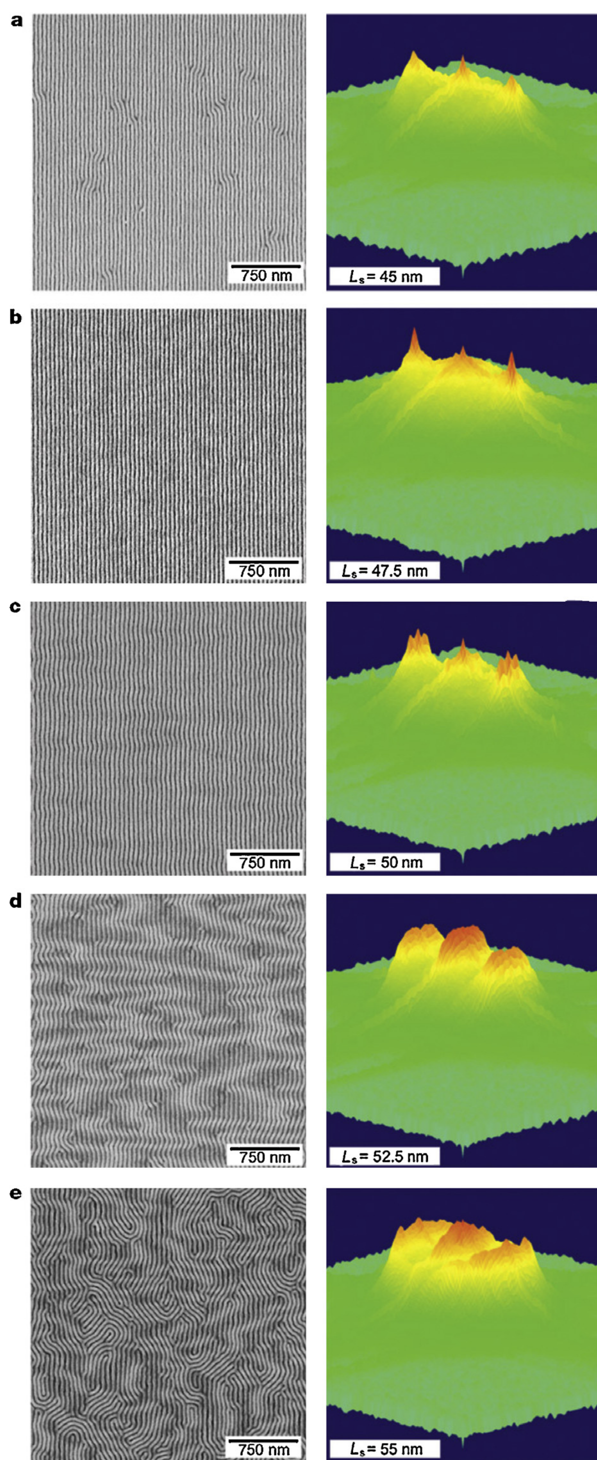

Fig. 2. Top-down SEM images and corresponding Fourier transform analysis of PS-*b*-PMMA copolymer films (L_0 = 48 nm, film thickness of 60 nm) on chemically patterned surfaces. The pattern periods, L_s, are (a) 45; (b) 47.5; (c) 50; (d) 52.5; and (e) 55 nm. The area of each SEM image corresponds to a 3 μm × 3 μm region of block copolymer domains. Ref. [14], Copyright 2003. Reproduced with permission from the Nature Publishing Group.

is controlled by the composition of the random copolymer, which is varied from 50:50 (neutral) to 100:0 (PS preferential). For each composition of the random copolymer brush, they studied the self-assembly of block copolymer domains on the underlying surface pattern with various periods, L_s = 40 nm, 42.5 nm, 45 nm, 47.5 nm, 50 nm, and 52.5 nm (Fig. 3). Block copolymer domains on the substrate patterned with the PS-*r*-PMMA 50:50 brushes only show registration and order approaching perfection when $L_s \cong L_0$ = 48 nm. Even in this optimal case there remains a considerable density of dislocation defects after a long time of annealing. As the deviation of L_s from L_0 increases, the order becomes increasingly worse with unregistered lamellae appearing at L_s = 45 nm and 50 nm. When L_s = 42.5 nm and 52.5 nm, areas with unaligned lamellae are significantly increased and at L_s = 40 nm no noticeable order with respect to the surface pattern is present. As the PS content in the PS-*r*-PMMA brushes is increased, the directing ability of the surface pattern is improved significantly, and accordingly the tolerance to the incommensurability of L_s and L_0 is increased. For the surface patterned by the pure PS brushes, the perfect epitaxial assembly is observed with a wide range of the pattern period 45 nm ≤ L_s ≤ 52.5 nm, and only an extremely low density of dislocation defects is present with L_s = 42.5 nm [104]. This study directly reveals that larger contrast in the interfacial energy enhances the directing ability of the chemical pattern and increases the window of permissible deviations between the periodicity, L_s of the chemical pattern and the bulk domain period, L_0, without losing the ability of defect-free assembly and registration.

In practice, a large tolerance to incommensurability between the period of the guiding pattern and the domain period of block copolymers is important for DSA, in particular, for the fabrication of device-oriented irregular structures, where the block copolymer domains have to form a variety of structures with different feature sizes [50]. For example, for a set of equally spaced bends with a pitch of L_s and a given angle of θ, the widest span at the bend corners is $L_s/\sin\left(\theta/2\right)$ which exceeds L_s by 40%. With the symmetric diblock copolymers, the work by Edwards et al. indicates that a period incommensurability within ±10% can be tolerated by the chemoepitaxial lithography leading to the defect-free lamellar pattern, which limits the application of AB diblock copolymers in the fabrication of irregular patterns [104]. One way to overcome this limitation consists in adding defectants – homopolymers [15] or nanoparticles [108] – to the block copolymer that locally swell the structure and allow for an adjustment of the domain spacing.

Recently, Ji et al. demonstrated that an ABA triblock copolymer tolerates a larger mismatch of the dimension of chemoepitaxial guiding patterns and the bulk copolymer periodicity than an AB diblock copolymer [107]. In the view of molecular architecture, symmetric ABA triblock copolymer can be conceived as a joint of two equivalent AB diblock copolymers at the ends of B blocks. Although ABA triblock copolymers self-assemble into a similar set of ordered phases and have similar phase diagrams as the corresponding AB diblock copolymers, the connection imparts ABA triblock copolymer with distinguished

properties [109]. ABA triblock copolymers exhibit a slightly lower χN_{ODT} than the corresponding AB diblock copolymer with half the molecular weight $N_{AB} = N/2$. The most prominent difference is that the central B blocks of the ABA triblock copolymer can form two distinct configurations: a bridge configuration, where the two A blocks, are located in apposite domains and a loop configuration, the two A blocks are located on the same side of the AB interface.

On one hand, the presence of bridges in ABA triblock copolymers significantly enhances the mechanical properties of their phase-separated structures. The ratio of loops and bridges varies with the domain spacing. Upon increasing the lamellar spacing from $L_s = L_0$ to $L_s = 1.5L_0$ the bridging ratio decreases from 41% to 17%. The compression modulus of the lamellar phase of triblocks, however, is very similar to that of the corresponding diblock system and free-energy dependence of stretching and compression

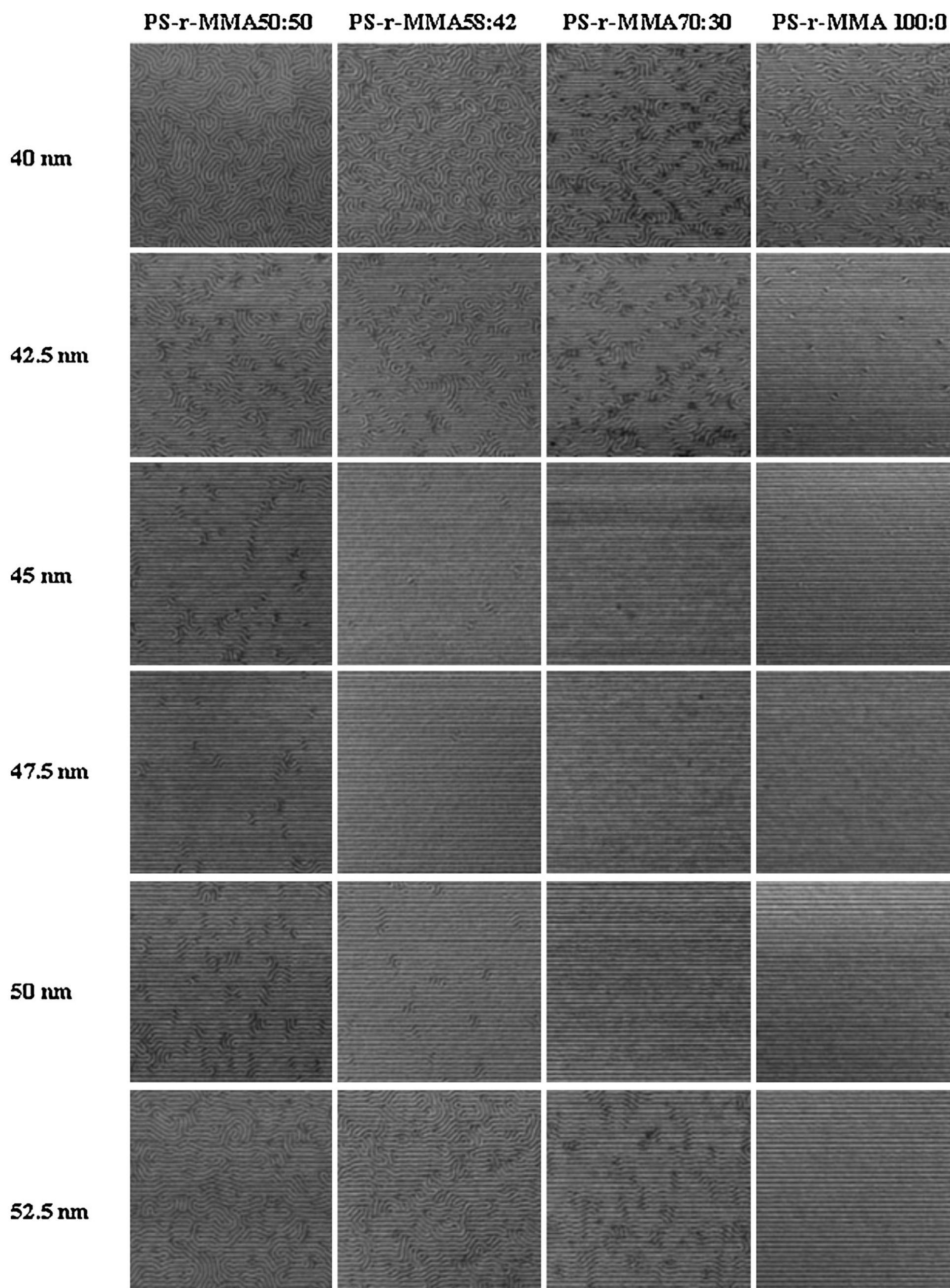

Fig. 3. SEM images of the surface-directed morphologies of lamella-forming block copolymer films ($L_0 = 48$ nm) on chemically patterned substrates with a variety of pattern periods L_s (40 nm < L_s < 52.5 nm) and composition of the random-copolymer brush used to create the chemical pattern. The micrographs depict areas of 2 μm square. Ref. [104], Copyright 2004. Reproduced with permission from the American Chemical Society.

Please cite this article in press as: Li W, Müller M. Directed self-assembly of block copolymers by chemical or topographical guiding patterns: Optimizing molecular architecture, thin-film properties, and kinetics. Prog Polym Sci (2015), http://dx.doi.org/10.1016/j.progpolymsci.2015.10.008

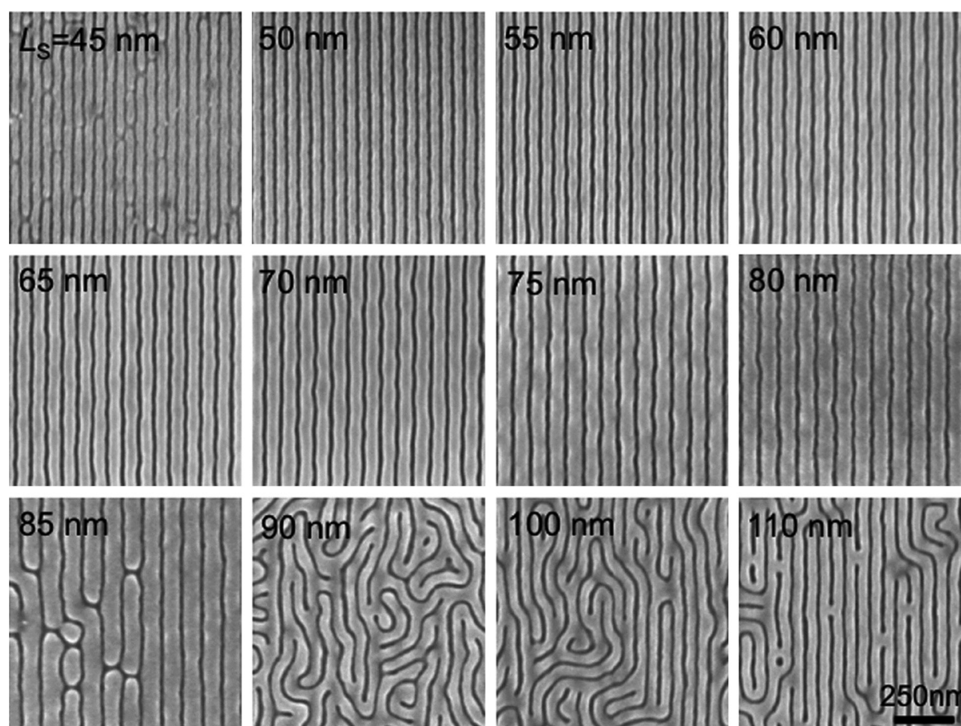

Fig. 4. Top-down SEM images of PMMA-*b*-PS-*b*-PMMA (M_n = 52–94–52 kg mol^{-1}) triblock copolymer thin films on chemical patterns with periods of 45–110 nm with a 5 nm increment. PMMA-*b*-PS-*b*-PMMA lamellar domains expand up to 55% (80 nm) and contract less 13% (45 nm) on chemical patterns in thin films. Ref. [107], Copyright 2012. Reproduced with permission from the American Chemical Society.

is nearly symmetric. On the other hand, loops do not contribute to the intrinsic curvature of the AB interfaces [110,111] whereas the two shorter A blocks bend the internal AB interface toward the B domain in order to enlarge the available volume and reduce the stretching of the end blocks [19,112]. Therefore, in contrast to the corresponding symmetric AB diblock copolymers, interfaces in the compositionally symmetric triblock copolymer system possess a spontaneous curvature. The consequences of this effect can be clearly seen in Fig. 4 where one exclusively observes broken domains of the middle B block but not of the A domains formed by the end blocks on top of chemical substrate patterns with $L_s/L_0 > 1$.

Ji et al. have studied the self-assembly of lamella-forming PMMA-*b*-PS-*b*-PMMA triblock copolymers (M_n = 52–94–52 kg mol^{-1}) with a domain period of L_0 = 51.5 nm on chemically patterned surfaces composed of alternating patterned PS brushes and silicon oxide stripes, with a variety of periods from L_s = 45 nm to 110 nm (Fig. 4) [107]. They have observed defect-free lamellar patterns with L_s = 50–80 nm, and these experimental observation have been additionally corroborated by coarse-grained simulations. Moreover, Ji et al. have also investigated the self-assembly of ABA triblock copolymers on chemical patterns comprised of equally spaced bends (see Fig. 5) with three bending angles 135°, 90°, and 45°, respectively [107]. ABA triblock copolymers perfectly replicated the chemical substrate pattern for bend angles of 135° and 90°, and defects occurred at the bending corners for the smallest angle of 45°. In marked contrast,

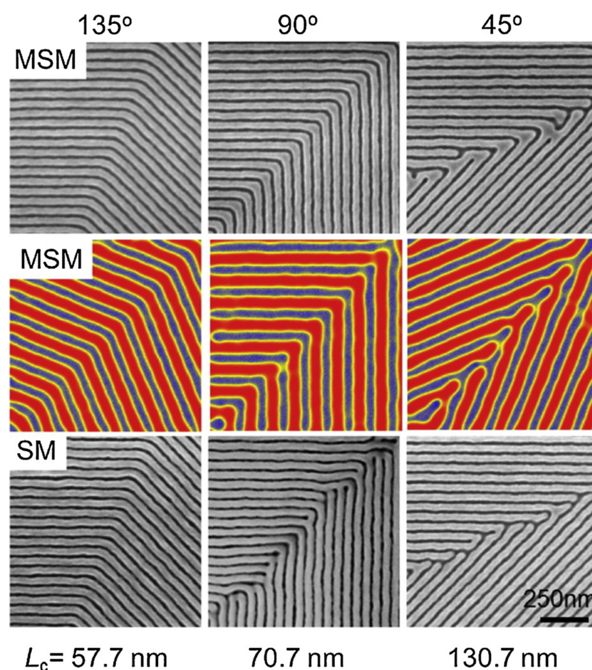

Fig. 5. Top-down SEM images of thin films of PMMA-*b*-PS-*b*-PMMA (M_n = 52–94–52 kg mol^{-1}) triblock copolymers and PS-*b*-PMMA (M_n = 52–52 kg mol^{-1}) diblock copolymers and images from MC simulations of the triblock copolymers on chemical patterns with 45, 90, and 135° bend geometries. Ref. [107], Copyright 2012. Reproduced with permission from the American Chemical Society.

pure AB block copolymer exhibits perfect registration only for the largest angle of 135° on top of similar chemical patterns.

In brief, DSA of pure AB diblock copolymers is able to replicate structures that closely match the symmetry and length scale of bulk morphologies, i.e., lines and spaces for lamellar-forming diblocks. The tolerance with respect to a mismatch between the symmetry or dimension of the guiding patterns and the equilibrium bulk morphology of the block copolymer is quite limited. This tolerance can be augmented by increasing the contrast in interfacial energies of the guiding pattern or using more complex copolymer materials (e.g. ABA triblock copolymers or blends). The latter finding suggests that small change to molecular architecture may give rise to significant differences in DSA performance. Thus, optimizing the molecular architecture (e.g. using multiblock copolymers) one might improve DSA and widen its application perspectives.

2.2. Multiblock copolymers

Other geometrically simple patterns targeted by DSA are 2D hexagonal structures formed by perpendicularly standing cylinders or single-layer thick spheres of compositionally asymmetric diblock copolymers. These structures find applications in fabricating quantum dot arrays for lasers [113] or high-density magnetic domains for storage media [114–116]. Both chemoepitaxy [17,60,102] as well as graphoepitaxy [16,20,47,48,117,118] techniques have been developed to fabricate defect-free hexagonal cylinder domains. However, square arrays, instead of hexagonal arrays, are more compatible with semiconductor integrated circuit design standards. The fabrication of square arrays, which are not an equilibrium phase of AB diblock copolymers or even other known AB-type block copolymers, such as ABA triblock or AB_n miktoarm copolymers [109,119,120], is a challenge.

Various approaches have been attempted to generate a square array of patterns with asymmetric diblock copolymers [63–65,121–123]. Hur et al. have conducted numerical two-dimensional (2D) SCFT calculations on the self-assembly of AB diblock copolymers or copolymer/homopolymer blends laterally confined in square wells aiming to obtain square lattices of standing-up cylinders [64]. Using pure diblock copolymers, a square 3×3 lattice of nine cylinders has been stabilized by using a slow thermal annealing process and optimizing the confining conditions of the square well, e.g. the surface interactions and the well size. This observation was confirmed by subsequent cell dynamic simulations: the 3×3 square array of cylinders is produced, while the 4×4 array becomes twisted [64,123]. This finding suggests that larger square lattice cannot be achieved by graphoepitaxy of diblock copolymer systems. The reason is that the tetragonal structure benefits from confinement geometry and only for a relatively small system this square-favoring surface free energy can compensate the bulk free-energy difference between the square structure and the hexagonal packing that corresponds to the equilibrium structure without confinement. A 4×4 square lattice of sixteen cylinders can be formed in a mixture of the copolymer with a homopolymer that is comprised of the same segments as the majority component of the diblock copolymer if the composition of the blend and the length ratio of homopolymer to copolymer are optimized. In the blends, the homopolymer of the majority component non-uniformly distributes and segregates to regions that otherwise would be filled by highly stretched coronal blocks of the copolymers. This balance between the loss of translational entropy of the homopolymers and the conformational stretching entropy of the majority block decreases the total free-energy excess of the square structure. As the size of square well increases, the bulk preference for hexagonal order becomes dominant over the wall-induced preference of the tetragonal order, and drives the cylinder domains to form twisted hexagonal arrays. The 4×4 square lattice however is still much smaller than hexagonal arrays, which can be formed by AB diblock copolymers laterally confined in hexagonal wells [117].

Although the square lattice of cylinders is not achievable in unconfined pure AB diblock copolymers, it can be derived from the bcc spherical phase because the (1 0 0) plane of the bcc lattice exhibits tetragonal symmetry [122,124,125]. Ji et al. has demonstrated a new strategy based on this idea to fabricate square patterns from the self-assembly of sphere-forming diblock copolymers in thin films [122]. The critical issue is how to maintain the bulk bcc structures in thin films. The hexagonally close-packed (hcp) array is the preferred sphere packing of block copolymers in thin films with the preferential wetting of one of the blocks of the copolymer at the substrate and the free surface, whereas this structure transforms into the face-centered orthorhombic phase approaching the bcc phase with the (1 1 0) plane parallel to the substrate as the number of sphere layers in the film is increased from 5 to 23 [92,126]. Therefore block copolymer thin films with preferential surfaces are not suitable for this task. Instead, the self-assembly of sphere-forming block copolymers in thin films with neutral/non-preferential surfaces will meet the requirement for forming multiple layer bcc structures with the (1 0 0) plane at the surfaces if the film thickness is appropriate. Ji et al. have obtained bcc structures self-assembled from sphere-forming block copolymers in thin films with commensurate film thicknesses, nL_0, where n is an integer and L_0 is the dimension of the bcc unit cell in the bulk [122]. These bcc structures are constituted of $2n-1$ layers of spheres plus two layers of half-spheres located on the two non-preferential surfaces, where each layer of spheres exhibits a consistent square array. With the optimized film thickness and surface interactions, defect-free square patterns have been achieved by the directed self-assembly of sphere-forming block copolymers on top of square chemical patterns with periods $0.9L_0\leq L_s\leq 1.1L_0$. In addition, the perfect epitaxial assembly has also been demonstrated on rectangular spot patterns fabricating the corresponding rectangularly arranged spheres in the (1 0 0) plane.

Since the strategies of fabricating square patterns via the self-assembly of AB diblock copolymers exhibit some disadvantages, i.e., that only limited size of square arrays is achievable by graphoepitaxy and stringent conditions of film thickness and surface preference are required for

Please cite this article in press as: Li W, Müller M. Directed self-assembly of block copolymers by chemical or topographical guiding patterns: Optimizing molecular architecture, thin-film properties, and kinetics. Prog Polym Sci (2015), http://dx.doi.org/10.1016/j.progpolymsci.2015.10.008

the formation of square array of semi-spheres in thin films. Therefore, block copolymers with a more complex molecular architecture, which are able to form the cylinder phase with the tetragonal symmetry in the bulk, may offer alternatives. When one chemically distinct C block is added onto AB diblock copolymer, ABC triblock terpolymers are produced. Compared with AB diblock copolymers, ABC triblock terpolymers have more variables controlling their phase behavior, including variable molecular architectures (e.g. linear and star), three interaction parameters ($\chi_{AB}N$, $\chi_{AC}N$, and $\chi_{BC}N$), and two independent volume fractions (f_A, f_B, with $f_C = 1 - f_A - f_B$). Accordingly, ABC triblock terpolymers can self-assemble into a huge number of fascinating periodic phases [1]. Abiding experimental and theoretical studies have focused on exploring of intriguing ordered structures formed in triblock terpolymers [66,67,72–80]. Even for linear triblock terpolymers, in addition to the core–shell phases that exhibit similar space symmetries as those formed in AB diblock copolymers, there are many other distinct phases, which are categorized into two types according to the arrangement of interfaces, i.e. *non-frustrated* (alternative) phases and *frustrated* phases where the formation of A/C interfaces frustrates the block sequence of the polymer chain [72]. Example of *non-frustrated* phases formed by ABC terpolymers [66,67,75] include the A/C alternative spherical phase, where A and C spheres are arranged on the CsCl crystal lattice with the central majority block, B, filling the interstitial space. In the A/C alternative cylinder phase, A and C cylinders form an alternating checkerboard pattern in a matrix of the B block. A number of attractive frustrated phases include 2D knitting patterns [74] and a variety of supercylinder phases where each cylinder is decorated by distinctive substructures, e.g. spheres, perforated lamellae, and single/double/triple helices [73].

From the point of view of block copolymer lithography, the A/C cylinder phase formed by ABC linear triblock terpolymers or equivalent block copolymer materials, which consists of independent square array of A or C cylinders while the two alternating square arrays co-form a unique square lattice with a square root of two times smaller period, is particularly suitable for fabricating square patterns. Early in 1992, the square array of cylinder phase was observed with polyisoprene-*b*-poly(2-vinylpyridine)-polystyrene (PI-*b*-P2VP-*b*-PS) by Mogi et al. [66], and it was also achieved in a blend system of AB and B′C diblock copolymers in which the B and B′ blocks interact by finely tuned hydrogen bonding by Tang et al (see Fig. 6) [121]. In recent years, a sequence of experiments by the research group of Ross have been devoted to develop strategies aiming at manufacturing defect-free square domain patterns from the directed self-assembly of ABC linear triblock terpolymers. Chuang et al. first templated the self-assembly of a PI-*b*-PS-*b*-PFS (polyferrocenylsilane) triblock terpolymers/PS homopolymer blend, which exhibits a wider process window for forming square patterns consisting of alternating PI and PFS cylinders oriented perpendicular to the substrate within a PS matrix than the pure triblock terpolymer, by trenches with untreated and PS-brush grafted wall surfaces, respectively [127]. Well oriented and ordered square arrays of PFS cylinders with 90° and 45° orientations of the lattice vector with respect to the trench edge are achieved in the trenches with the two surface conditions, respectively. In this templated self-assembly, the film thickness plays a critical role. Films are rather thin and their thickness is finely tuned, whereas a larger film thickness leads to the formation of in-plane cylinders.

In a subsequent work, Ross and coworkers utilized additional strategies to improve the ordering of square cylinder patterns formed by triblock terpolymer/homopolymer blend and applied an optimized combinatorial strategy to the directed self-assembly on two distinct patterned substrates: rectangular sidewalls and periodic nanoposts [128]. In order to orient the PI or PFS cylinders perpendicular to the substrate in thin films, the substrate is grafted with a brush layer that chemically differs from all three blocks of the triblock terpolymer aiming at producing a non-preferential surface for all three blocks. Moreover, the polymer film is solvent annealed in a vapor with a fine-tuned swelling ratio that modulates the chain mobility and interaction parameters. Under these tailored conditions, highly ordered square arrays of cylinders standing on homogeneously P2VP- or PEO-brushes grafted substrates are fabricated with average grain sizes larger than a micrometer. Afterwards, the well ordered square patterns are registered by the rectangular sidewalls and periodic nanoposts, where the well surfaces and the bottom substrate are independently chemically functionalized in order to improve the registration quality (see Fig. 7). Single-grain square patterns with an excessively low density of defects are produced on the two patterned substrates. These studies demonstrate the application potential of copolymer architectures beyond AB diblock copolymers in DSA.

Defects in square patterns, which are fabricated by DSA of ABC triblock terpolymers confined by rectangular sidewalls, are more pronounced at the corners of the cage because a corner frustrates the formation of bridge between neighboring A and C cylinders. This problem does not occur in hexagonal patterns formed by the self-assembly of AB diblock copolymers in hexagonal wells [117,118], and it can be circumvented by using AB-type copolymers, whose molecular architecture has been purposely designed as to yield a stable cylinder phase with square symmetry in the bulk. For instance, SCFT calculations predict that AB-type block copolymers with a pitchfork-like dendritic architecture self-assemble into such a phase of square symmetry [129]. Since modern synthesis techniques rapidly develop, a large multitude of multiblock copolymers with increasingly complex architectures, including two-component AB-type and three-component ABC-type terpolymers [4,130,131], have been synthesized. These diverse architectures significantly enrich the self-assembly structures of block copolymers. To date, SCFT calculations have predicted that morphologies, which are only metastable in AB diblock or ABA triblock copolymers, become stable in AB two-component copolymers with designed architectures, including the A15 and σ spherical phases in AB_n star copolymers [119,120] and the perforated lamellar phase in AB_n and comb copolymers [132]. These types of

Please cite this article in press as: Li W, Müller M. Directed self-assembly of block copolymers by chemical or topographical guiding patterns: Optimizing molecular architecture, thin-film properties, and kinetics. Prog Polym Sci (2015), http://dx.doi.org/10.1016/j.progpolymsci.2015.10.008

copolymer materials offers an appealing prospect for fabricating device-oriented structures.

However, it is impracticable to search for a desired ordered phase by simply exploring the vast architecture pool that indeed consists of infinite number of candidate architectures with varying block numbers and topologies. Without any valid guiding principle, the self-assembly of block copolymers with a variety of architectures may become only a Pandora's box. Spherical phases formed in block copolymers resemble the space symmetries as atomic crystals, e.g. single-component crystals of fcc, bcc, and A15 self-assembled by two-component copolymers, and binary crystals of CsCl self-assembled by ABC linear triblock terpolymers. However, significantly fewer types of crystal structures have been observed in sphere-forming block copolymers than in atomic crystals. In particular, the only stable binary spherical phases formed by ABC linear triblock terpolymers is the CsCl-type, whereas there is a large number of binary atomic crystals, e.g. tens of binary ionic crystals. Very recently, Xie et al. have proposed a useful guiding principle of the molecular design of multiblock terpolymers for stabilizing distinct stable binary crystal spherical phases. Abiding by this design principle, $B_1AB_2CB_3$ pentablock or AB_2CB_3 tetrablock terpolymers are designed, where A and C blocks independently form spheres acting as *artificial macromolecular atoms*, *AMAs* in a matrix of B blocks. The effective bond length and average magnitude of coordinate numbers (CNs) of AMAs are tuned by the relative length of the middle B_2 block to the fixed total B composition, and the asymmetry of CNs between A and C AMAs is tuned by the molecular asymmetry regulated by the relative length between two terminal B blocks (Fig. 8). Along the first path, the pentablock terpolymer $B_1AB_2CB_1$ is symmetric and hence forms the binary crystal phases of equal CNs. As the relative length of the middle B_2 block decreases, the distance of A/C spheres (or the dimension of the unit cell), i.e. the effective bond length, has to be reduced in order to release the stretching of the B_2 block. Because of the fixed composition of the three B blocks, the sphere size decreases as the decrease of the bond length, and in turn, it induces the A/B or B/C interfacial energy to be raised, if the crystal lattice is maintained. When the penalty of interfacial energy becomes disastrously high, it will drive the crystal lattice to transfer into a new one with a lower CN which is favorable to form larger spherical domains. Accordingly, a sequence of stable crystal phases, from CsCl (CN = 8), NaCl (CN = 6), ZnS (CN = 4), to α-BN (CN = 3), is predicted with the self-assembly of $B_1AB_2CB_3$ pentablock terpolymers when gradually reducing the relative length of the middle B_2block while fixing the total B composition.

Whereas along the other paths, the terpolymer molecules, AB_2CB_3 tetrablock or $B_1AB_2CB_3$ pentablock

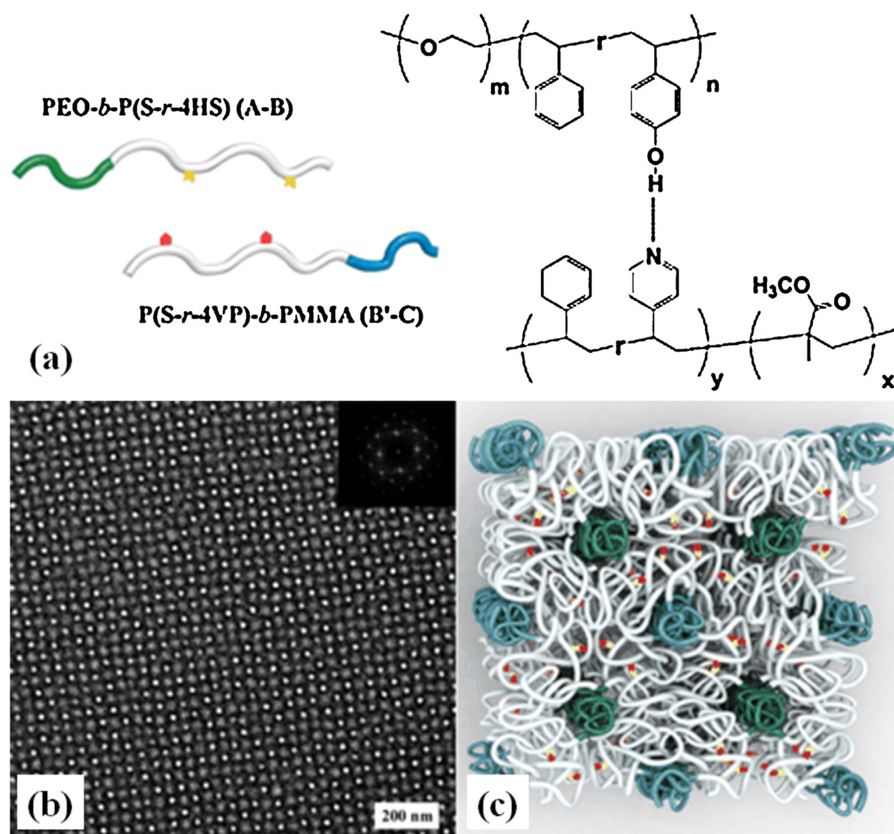

Fig. 6. (a) Supramolecular blend of PEO-*b*-P(S-*r*-4HS) (A–B) and P(S-*r*-4VP)-*b*-PMMA (B′–C) diblock copolymers that the B and *B*' blocks have controllable hydrogen bonding interactions. (b) TEM image and associated Fourier transform (inset) of a solvent-annealed blend film of supramolecular block copolymers in (a). (c) A cartoon illustrates proposed chain packings. Ref. [121], Copyright 2008. Reproduced with permission from AAAS.

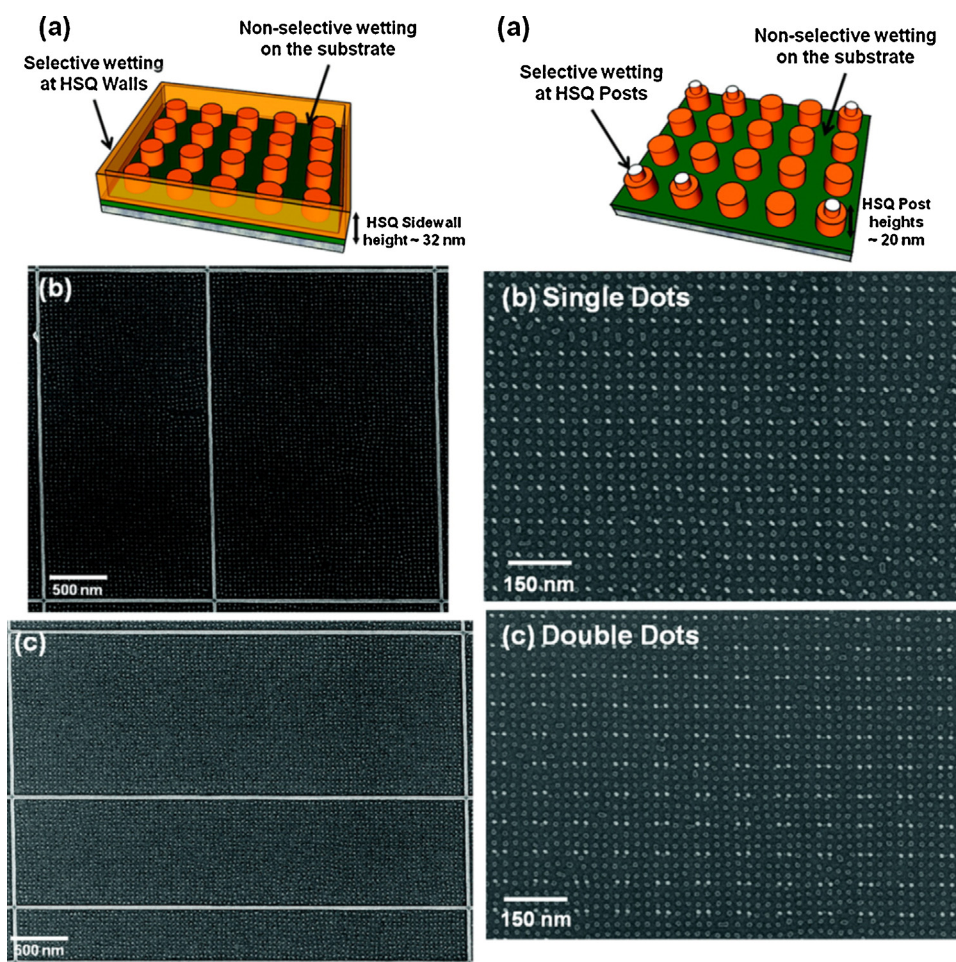

Fig. 7. Left column: Highly ordered square arrays formed from the directed self-assembly of PI-*b*-PS-*b*-PFS triblock terpolymer films by rectangular sidewalls. (a) Schematic of a square array of microdomain triblock terpolymer films within a topographical template with preferential PFS brush coated sidewalls and non-preferential PEO brush coated horizontal surfaces. (b) and (c) SEM images of oxidized PFS domains in (b) 1.5 μm and 2 μm × 3 μm and (c) 0.5 μm, 1 μm, and 1.5 μm × 4 μm templates. Right column: (a) Schematic and (b and c) SEM images of ordered square arrays formed on a sparse 2D lattice of nanoposts (b) 88 nm × 132 nm single posts and (c) 44 nm spacing double posts (brighter dots). Similarly, The substrate surface is functionalized with a PEO brush layer and the post sidewalls are coated with PFS brush layer. Ref. [128], Copyright 2011. Reproduced with permission from the American Chemical Society.

with nonequal terminal B blocks, become asymmetric, and thus self-assemble into binary crystal phases with unequal CNs where the asymmetry of CNs is determined by the asymmetric degree of the molecules but the average magnitude of CNs, $\overline{CN}$, is determined by the relative length of the middle B_2 block. Many stable binary crystal phases, e.g. $A1B_2$ ($\overline{CN} = 8$), Li_3Bi ($\overline{CN} = 7$), CaF_2 ($\overline{CN} = 16/3$), Nb_3Sn(A15) ($\overline{CN} = 6$), TiO_2 ($\overline{CN} = 4$), ReO_3 ($\overline{CN} = 3$), and α-Al_2O_3 ($\overline{CN} = 24/5$), are predicted by SCFT calculations. In addition, a lot of novel ordered non-spherical phases are explored, e.g. helical supercylinder phases and hierarchical gyroid phases. In particular, there are a variety of cylinder (2D crystal) phases with plane symmetries, *p4mm*, *p3m1*, *p6mm*, and *c2mm* (there are two distinct phases with the same plane symmetry, *p4mm* or *p6mm*), which are applicable in the patterning technique of DSA.

This theoretical study serves as a good starting point for the establishment of a platform for the fabrication of desired structures via designed block copolymers abiding by valid design principles. Of course, the guiding principle to tune the effective bond length and CNs in binary crystal phases is not the only one, and more useful design principles can be inferred from systematically exploring and rationalizing the intriguing multitude of bulk structures that simple two-component AB copolymer materials can form when one allows for blending or alternative chain topologies, (i) control of the spontaneous curvature of internal interfaces by molecular architecture [111,112,119,120], (ii) mitigation of packing frustration by polydispersity [133–136]. For example, branching feature in AB_n star copolymers increases the tendency of forming curvature toward A domains in order to maximize the entropy of chain configurations, and hence expands the phase region of spheres toward the direction of the symmetric composition, where the A15 and σ phases become stable instead of the classical bcc phase [119,120]. Combining these rational guiding principles enables the self-assembly of designed block copolymers

Please cite this article in press as: Li W, Müller M. Directed self-assembly of block copolymers by chemical or topographical guiding patterns: Optimizing molecular architecture, thin-film properties, and kinetics. Prog Polym Sci (2015), http://dx.doi.org/10.1016/j.progpolymsci.2015.10.008

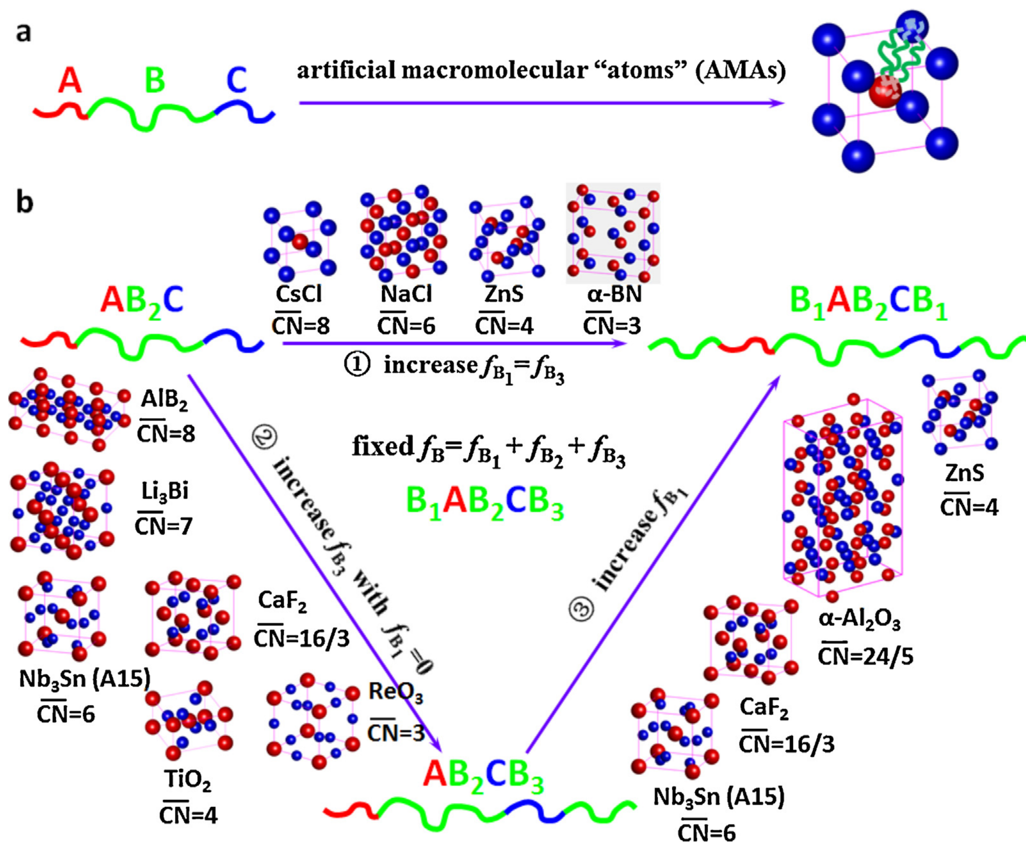

Fig. 8. Design principle of multiblock terpolymers for binary soft mesocrystals. (a) Artificial macromolecular "atoms" (AMAs) self-assembled by linear ABC triblock copolymers pack into the CsCl crystal lattice. (b) AMAs formed by multiblock terpolymers can be programmed to assemble into a variety of crystallographic arrangements by tailoring the polymer architectures. Three possible paths are demonstrated to design series of mesocrystals with varying magnitude and asymmetry of coordination numbers (CNs) by tuning the relative lengths among B blocks while keeping the total B component fixed. Ref. [85], Copyright 2014. Reproduced with permission from the American Chemical Society.

into desired structures, and thus widens the application spectrum of block copolymers in the DSA patterning technique.

2.3. Blending and supramolecular polymer materials

Blending different polymer molecules is a convenient strategy for designing polymer materials with distinct properties that cannot be achieved by the corresponding pure components. In microphase-separating copolymer systems, blending can modify multiple properties – (i) domain dimension (i.e., by swelling), (ii) average volume fraction of A and B segment species (i.e., effective composition, f, of the corresponding pure copolymer system), and (iii) molecular weight polydispersity – and thus vary the phase behavior, e.g. stabilizing novel ordered phase or even lead to macrophase separation.

One of the most intensively studied blends is simply prepared by mixing a diblock copolymer with its constitutive homopolymers. The phase behavior of this ternary blend, which has been studied by SCFT [87–89,109], simulations [90,137], and experiments [86,138–143], is complicated because of the interplay between macro- and microphase separation and the importance of fluctuation effects. AB diblock copolymers act as compatibilizer and their addition to immiscible A and B homopolymer blends can generate a stable macroscopically homogeneous mixture at low incompatibility. At higher χ^N, the ternary blend conceptually mimics the behavior of the well-known mixture of oil, water, and amphiphilic surfactant, and it is able to form an intriguing microemulsion-like morphology comprised of undulating interfaces. Thermal fluctuations give rise to this disordered morphology that forms for thermodynamic parameters where the bending rigidity and tension of the copolymer-ladder AB interfaces nearly vanishes [109,111]. The distance between interfaces diverges in an unbinding transition [87]. Within mean-field theory this region corresponds to the vicinity of a Lifshitz point whereas fluctuations result in the formation of a bicontinuous microemulsions [86,90,144]. This structure is believed to exhibit unique and useful mechanical, electrical, optical, or barrier properties.

If only a small amount of homopolymers is added to a block copolymer melt, the domain dimension and effective composition will be modified by selectively swelling domains that prefer the homopolymers [89,107,145–147]. As synthesizing block copolymers with various precise compositions aiming at forming desired ordered phases is difficult and costly, adding homopolymers is an inexpensive strategy to control the effective composition and

domain size within a limited range. As discussed in the previous subsection, PS homopolymers are added into the PI-*b*-PS-*b*-PFS triblock terpolymers to facilitate the formation of the square cylinder phase [127,128]. The work by Stoykovich et al. reveals that the directed self-assembly of ternary blends of diblock/homopolymers on chemically patterned substrates has an improved tolerance toward a mismatch between the characteristic dimension of guiding pattern and bulk periodicity of copolymer systems [145]. Hayashida et al. have successfully demonstrated the formation of a variety of polygonal tiling patterns by blending a small amount of A or B homopolymers into ABC star-shaped terpolymers to tune the compositions [147].

In the self-assembly of pure AB diblock copolymers, two important competing factors dictate the domain geometries of ordered phases, i.e. the average mean curvature and the standard deviation of mean curvature that minimize the interfacial tension and the packing frustration of polymer chains, respectively [58,148]. Especially, in complex phases such as the perforated lamellar (PL), the bicontinuous gyroid, or the diamond phase, some macromolecules excessively stretch to fill space uniformly, and the second factor becomes more pronounced leading to more stable gyroid phase rather than the PL and diamond phases. The addition of homopolymers to the majority domain of the PL phase and to the minority domain of the diamond phase reduces this excessive stretching, i.e. mitigates the packing frustration of polymer chains, thereby stabilizing the corresponding phases [89,146,148–150].

Additionally, similar to surfactants that enrich at interfaces and thereby lowering the interfacial tension [15,50,107], homopolymer additive plays a critical role acting as “defectants” [68] in stabilizing non-bulk structures in pure block copolymer systems by preferentially aggregating at high-stress regions and hence lowering the excess free energy. For instance, the addition of homopolymers to bulk copolymer systems can alter the probability of defect structures (e.g. by lowering the cost of grain boundaries) [151].

The defectant property of homopolymers has been particularly useful for the fabrication of irregular or aperiodic structures, where domain features are usually highly nonuniform [15,50]. Increased packing frustration of copolymer chains in highly nonuniform domains may impede perfect DSA into irregular structures. In bend structures, noticeable imperfections are present at small angles (cf. panels corresponding to 90° and 45° in Fig. 5) [107]. These imperfections can be reduced or even eliminated by blending certain amounts of corresponding A and B homopolymers into the copolymer material. Experiments and simulations have proven the success of this strategy by directing the self-assembly of a PS/PMMA/PS-*b*-PMMA ternary blend guided on chemically patterned substrate [50] into a set of device-oriented structures like isolated and nested jogs as well as arrays of T-junctions.

When aiming at replicating different, spatially extended patterns on the same waiver (e.g. structures that resemble electronic circuits) each pattern requires its own concentration and molecular architecture of “defectants”. Although a “defectant” *mixture* may be able to replicate a mixed patterns in equilibrium, this strategy relies on the slow sorting of “defectants” to the respective patterns. If the concomitant time scale of diffusive sorting were longer than the time scale of spontaneous self-assembly, many defects would form during the initial stages of structure formation and the elimination of these defects is a protracted process. Supramolecular polymer materials, in which bonds form and break reversibly, mitigate this challenge because they constitute *universal* “defectants” [68]. The supramolecular material rapidly adopts to the DSA guiding pattern by locally and reversibly generating the “right defectant mix” that allows the copolymer self-assembly to form irregular structures. This local response has two advantages: First, one does not need to finely tune the molecular characteristics of the defectant mix, e.g. the composition or molecular weight of the homopolymer additives. Second, it does not rely on the slow, diffusive sorting of the “defectants” to their respective patterns but they are generated in place.

Polymeric supramolecules formed by complexing block copolymers with specific functional groups via special chemical interactions provide a powerful platform to fabricate hierarchical nanostructures with several length scales that allow straightforward tailoring of hierarchical order–disorder and order–order transitions and the concurrent tuning of functional properties [152]. Fig. 9 presents such a molecular complexation, PS-*b*-P4VP $(MSA)_{1.0}(PDP)_{1.0}$, which is built up by stoichiometrically protonating the minority block P4VP with methane sulfonic acid (MSA) to form $P4VP(MSA)_{1.0}$, and then complexing pentadecylphenol (PDP) to it by hydrogen bonding. At a low temperature, $T < T_{ODT_C} \approx 110\,^{\circ}C$, the full complexation of both MSA and PDP to P4VP leads to the volume fraction of the complexed block $f_{P4VP(MSA)_{1.0}PDP_{1.0}} = 0.40$, and hence the block copolymers self-assemble into a hierarchical lamellar structures with two distinct length scales, where there is sub-lamellar domains with a small period $L_c \approx 4.8$ nm aligned perpendicularly to the major PS layers that are formed by the further microphase separation between the subgroups PDP and the backbones $P4VP(MSA)_{1.0}$ (see Fig. 9(A)). As the hydrogen bonding in the complexation PS-*b*-P4VP $(MSA)_{1.0}(PDP)_{1.0}$ is sensitive to temperature, the hierarchical lamellar structure in Fig. 9(A) transfers to the normal lamellar layers in Fig. 9(B) when the second complex layer structure undergoes an ODT at $T_{OCT_C} = 100\,^{\circ}C$,. When increasing temperature further to be above 150 °C, an interesting order–order transition from the lamellar phase to the hexagonal cylinder phase in Fig. 9(C) is occurred because dissociated PDP molecules become miscible with PS at increased temperatures and thus their diffusion into the majority PS domains reduces the volume fraction of the P4VP-contained domains. Accordingly, the temperature response of the phase behavior directly tunes the functional properties, e.g. the conductivity which is mainly contributed by the backbone block $P4VP(MSA)_{1.0}$. In the hierarchical lamellae, the conducting nanoscale slabs are separated by insulating PS and PDP domains, and therefore the macroscopic conductivity is small because of the high anisotropic alignment in bulk morphologies. The ODT inside the P4VP-containing layers results in an order of magnitude increase in conductivity because disordered

Please cite this article in press as: Li W, Müller M. Directed self-assembly of block copolymers by chemical or topographical guiding patterns: Optimizing molecular architecture, thin-film properties, and kinetics. Prog Polym Sci (2015), http://dx.doi.org/10.1016/j.progpolymsci.2015.10.008

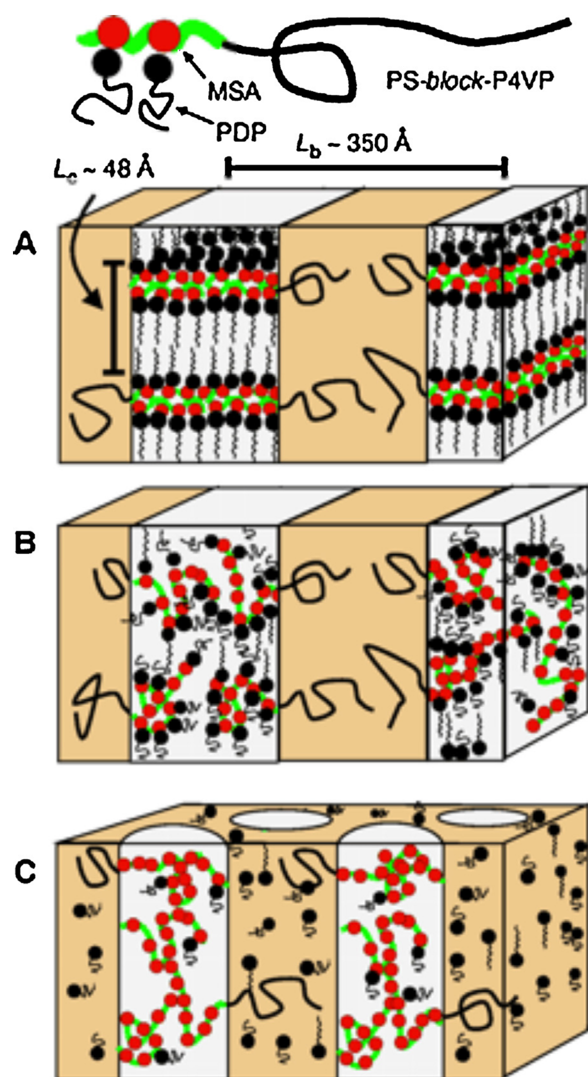

Fig. 9. Schematic illustration of the self-organized structures of supramolecular diblock copolymers PS-*b*-P4VP(MSA)$_{1.0}$(PDP)$_{1.0}$. (A) Hierarchical lamellar morphologies composed of major PS layers and composite layers consisting of alternating minor layers of P4VP(MSA)$_{1.0}$ and PDP for T < $T_{\mathrm{ODT_C}}$. (B) Simple lamellar morphologies composed of alternating PS and disordered P4VP(MSA)$_{1.0}$(PDP)$_{1.0}$ lamellae for $T_{\mathrm{ODT_C}} < T < T_{\mathrm{OOT_C}}$. (C) Hexagonal cylinders with disordered P4VP(MSA)$_{1.0}$(PDP$_x$) (with $x \ll 1$) cylinders within the mixing PS-PDP matrix for $T_{\mathrm{ODT_b}} < T$. Ref. [152], Copyright 1998. Reproduced with permission from AAAS.

lamellar morphologies exhibit near bicontinuous network structures [22,23]. Finally, above the OOT leading to the cylinder phase, the conductivity drops down because the connection of bulk cylinder morphologies is worse than that of bulk lamellar morphologies.

An alternative supramolecular architecture are quasi-block copolymers that consist of AB diblock copolymers and supramolecular B segments. The latter can reversibly bond to any B terminus on the copolymers or B oligomers. Thus, a polydisperse blend of B homopolymers, AB diblock molecules, and ABA triblock copolymers is formed [153]. As illustrated in Fig. 10 such a *single* copolymer material replicates different irregular patterns without defects like, e.g. perpendicularly crossing lines (square, tic-tac-toe pattern) that differ by up to 50% in their periodicity. Such a pattern poses a DSA challenge for several reasons: (1) Structures of square symmetry are found in the bulk of the material, (2) the continuous matrix phase (lines) is formed by the minority component, and (3) the line-crossing gives rise to significant packing frustration because the distance between the internal AB interfaces varies. The local adjustment of the stoichiometry of the material is critical for successful DSA. For the specific example, the composition of the quasi-block copolymer material is 90% triblocks, 5% diblocks, and 5% homopolymers. Unexpectedly, the pattern with the larger feature size contains shorter ABA triblocks than the small-scale structure because the shorter copolymers locally swell of line-crossings [68]. This system constitutes also another illustration of a complex, two-component macromolecular architecture capable of forming a structure with square symmetry.

3. Control film properties

Spin-coating block copolymers into thin films is a fundamental step for many practical applications such as DSA patterning techniques. Accordingly, the equilibrium phase behavior of block copolymers confined into thin films has been extensively studied by experiment, simulation, and theory [6,91,93,154–164].

Spin-coated films are bounded on one side by air or vapor, i.e., the top surface is deformable. For lying structures, e.g. lamellar sheets or cylinders oriented parallel to the surfaces, experiments observe the formation of terraces [154,165]. The top film surface is not flat but, instead, the system laterally separates into extended, macroscopic areas of different thickness ("islands" and "holes"). "Islands" and "holes" laterally coexists and the corresponding film thickness adjusts accordingly (approximately to multiples of the bulk periodicity).

For quasi-two-dimensional structures, which are uniform across the film thickness (e.g. standing lamellae or cylinders that are most relevant for DSA), the film remains laterally homogeneous on macroscopic scales and the local deformability of the free surface is less important because the free energy of the internal AB interfaces of low-χ mixtures is typically an order of magnitude smaller than the surface tension between polymer and vapor.

In addition to the geometry of confinement, the interaction energy of the polymer components with the confining surfaces is crucial. In addition to the surface interactions, which are also present for mixtures of small molecules, there are additional entropic effects associated with the orientation of the extended macromolecules and the enrichment of chain ends in the narrow interface between the supporting substrate or vapor and the polymer melt [155,156,159]. These subtle entropic contributions to the free energy of the confined system may affect the orientation of the structures [166]. Note that geometric confinement and surface interactions do not only dictate the equilibrium thermodynamic properties but additionally exert a pronounced influence on the spinodal kinetics during the initial stages of structure formation [98] (cf. Section 4).

Please cite this article in press as: Li W, Müller M. Directed self-assembly of block copolymers by chemical or topographical guiding patterns: Optimizing molecular architecture, thin-film properties, and kinetics. Prog Polym Sci (2015), http://dx.doi.org/10.1016/j.progpolymsci.2015.10.008

Even the phase diagram of a deceptively simple diblock copolymer in a thin film is determined by a multitude of variables that include the two standard parameters, χN and f, characterizing the equilibrium bulk behavior within mean-field-approximation, and at least three additional parameters parameterizing the confinement—the film thickness and the difference of surface tensions between the two components of the copolymer and the top of the film (air or vacuum) or the bottom substrate. As the components of copolymer are increased, e.g. ABC triblock terpolymers, or more additional molecules are incorporated, e.g. solvents or homopolymers, the parameter space rapidly expands.

In addition to the molecular architecture also the geometry of confinement can we tailored. The structures that form in a wedge-shaped confinement are illustrated in Fig. 11. Another popular geometry are cylindrical nanopores, which are relevant to the fabrication of contact-hole in semi-conductor industry and that give rise to a fascinatingly rich set of morphologies [167–169].

The stability of copolymer structures is determined by the combined effect of all factors—geometry and length scale of the copolymer bulk structure that is encoded in its molecular architecture, geometry of the confinement and interactions with the film surfaces. Aiming at fabricating targeted structures, one has to simultaneously optimize all these variables—this remains a big challenge for experiments alone. Usually the block copolymer phase behavior serves as the principal guide for experiments to fabricate desired structures. A variety of theoretical approaches have been employed to explore the phase behavior of distinct block copolymer materials in thin films, including coarse–grained Monte Carlo (MC) simulations[91,95,170–173], dynamic density functional

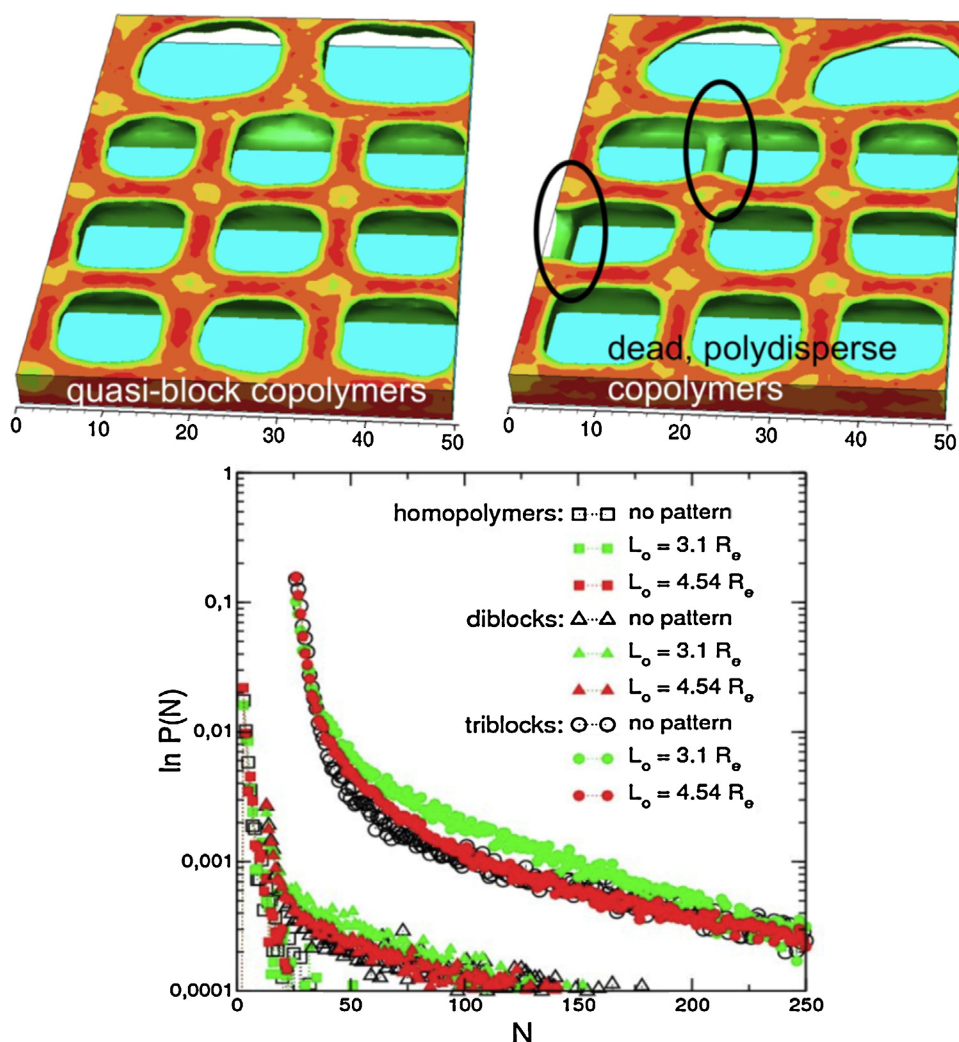

Fig. 10. DSA of quasi-block copolymers on a tic-tac-toe structure comprised of two periodicities. The quasi-block copolymer results in a morphology without defects (left image), while the kinetics of structure formation of a polydisperse blend of identical but frozen distribution of macromolecules results in two defects that are highlighted by ellipses in the right panel. The bottom figure depicts the length distribution of homopolymers, diblocks and triblocks in the quasi-block copolymer on a substrate without pattern and two square patterns with different periodicities, L_0. Ref. [68], Copyright 2010. Reproduced with permission from the American Physical Society.

Please cite this article in press as: Li W, Müller M. Directed self-assembly of block copolymers by chemical or topographical guiding patterns: Optimizing molecular architecture, thin-film properties, and kinetics. Prog Polym Sci (2015), http://dx.doi.org/10.1016/j.progpolymsci.2015.10.008

theory (DDFT) [162,174,175], single-chain-in-mean-field (SCMF) simulations [176–178], and SCFT [93,94,144,156]. Computer simulations and calculations are instrumental to explore the parameter space. Moreover, optimization strategies based on DDFT or SCFT have been utilized to reconstruct the three-dimensional volume structure from experimentally available two-dimensional surface information [179].

One of the important applications consists in fabricating free-standing lamellar stripes or hexagonal cylinders by the self-assembly of block copolymer thin films [14,15,180,181]. For controlling the orientation of domains, surface interactions and film thickness play a critical role. In principle, diblock copolymers in thin films with two neutral surfaces are able to self-assemble into perpendicular morphologies regardless of film thickness [156,159]. As long as there is only a small preference of the surface interactions, the competition between the perpendicular structures and others is dictated by the interplay of the surface interactions and the film thickness, which may frustrate laying structures. Large preferences of surface interactions, however, significantly reduce the phase region of perpendicular phases with respect to film thickness [159,162,174,175]. In experiments, neutral substrates can be prepared by chemical functionalizations [180,181], e.g. grafting random copolymer brushes that are composed of the same segment species as the block copolymers [180], whereas there is usually no simple strategy for neutralizing the free top surface except for replacing the surrounding air with an appropriate solvent vapor or vacuum. Thus block copolymers that contain the blocks with near equal surface tensions with respect to air – like the model diblock copolymer PS-*b*-PMMA – are particularly popular. More recently, top coats have been devised to neutralize the preference of the top surface for high-χ materials [182,183].

In contrast to neutral surfaces, preferential surfaces can alter the phase behaviors of block copolymer thin films more seriously not only breaking the translational symmetry normal to the surfaces but also changing the space symmetry by surface wetting and surface-induced ordering [93,94,162]. Already in the simple case that both preferential surfaces are homogeneous and identical, non-bulk structures can be readily formed. For example, varying the film thickness and surface preferences of a film of cylinder-forming copolymers, one observes spheres, perforated lamellae, and lamellae in addition to cylinder phases with various orientations in experiments and simulations [91,162]. Interestingly, experiments and concomitant DDFT simulations observe distinct morphologies in a *single* film of cylinder-forming ABA triblock copolymers with gradually varying film thickness (at steps between terraces) (see Fig. 11) [162]. Recently, SCFT calculations explored the phase diagram of AB diblock copolymer films confined by identical, B-attracting surfaces as a function of copolymer composition and film thickness (see Fig. 12) [93]. Twenty ordered morphologies are considered in this phase diagram. Increasing the copolymer composition, one observes a bulk-like sequence of equilibrium structures and the comparison to the bulk phase diagram highlights the impact of confinement on the OOTs. For instance, perforated lamellae are present not only in the region of the bulk gyroid phase but also in that of the bulk cylinder and bulk lamellar phases. As discussed in Section 2 an even richer behavior can be anticipated from more complex block copolymer architectures or in mixtures.

In DSA applications the surfaces are laterally inhomogeneous in order to guide the structure formation of the copolymer material. Ideally, the lateral symmetry and length scale of the guiding pattern and the bulk morphology coincide [101] (see Section 2 for further discussion) or

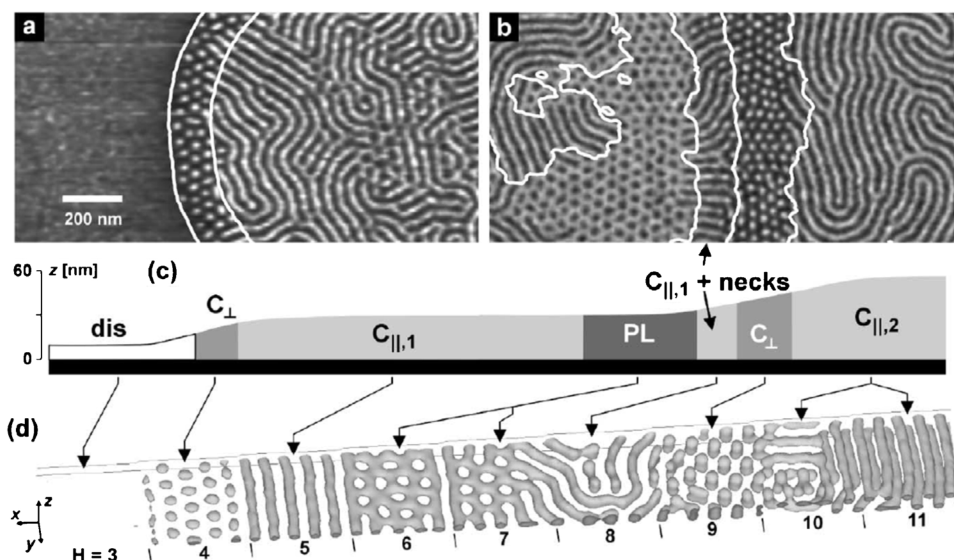

Fig. 11. (a and b) Tapping mode scanning force microscopy images of thin PS-*b*-PB-*b*-PS triblock copolymer films on silicon substrates after annealing in chloroform vapor. The surface is everywhere covered with an about 10-nm-thick PB layer. Bright (dark) corresponds to PS (PB) microdomians below the top PB layer. Contour lines calculated from the corresponding height images are superimposed. (c) Schematic height profile of films in (a and b). (d) Simulation of an $A_3B_{12}A_3$ triblock copolymer film in one large simulation box of [$352 \times 32 \times H(x)$] grid points with increasing film thickness $H(x)$ and preferential surfaces to the B component. Ref. [162], Copyright 2002. Reproduced with permission from the American Physical Society.

Please cite this article in press as: Li W, Müller M. Directed self-assembly of block copolymers by chemical or topographical guiding patterns: Optimizing molecular architecture, thin-film properties, and kinetics. Prog Polym Sci (2015), http://dx.doi.org/10.1016/j.progpolymsci.2015.10.008

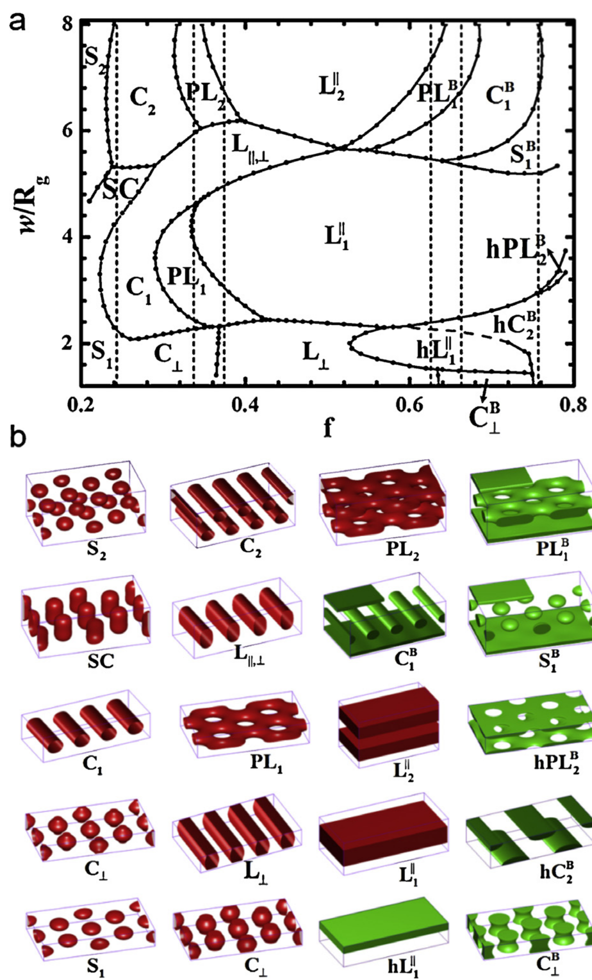

Fig. 12. (a) Phase diagram of AB diblock copolymer thin films of fixed $\chi N = 20$ with respect to the volume fraction of the A block and the film thickness, w, in units of R_g. Both surfaces have intermediate strength of attractive interactions to the B blocks. The dots are calculated phase transition points by SCFT, while curves are guides to the eye, indicating the phase boundaries. The dashed lines indicate the bulk phase transitions of AB diblock copolymers between sphere and cylinder, cylinder and gyroid, and gyroid and lamella. (b) Density isosurface plots of morphologies in the phase diagram. When $f_A < 0.5$, the isosurfaces of the A component are plotted in red color, and otherwise, the isosurfaces of the B component are plotted in green color. Ref. [93], Copyright 2013. Reproduced with permission from the American Chemical Society. (For interpretation of the references to color in this figure legend, the reader is referred to the web version of this article.)

alternatively the period of the guiding pattern is an integer multiple of the periodicity of the copolymer structure, i.e., the sparse guiding pattern dictates orientation and registration whereas the self-assembling material “fills-in” the small-scale structure (density multiplication [17]).

Differences between the bulk structure of the copolymer material and the guiding pattern are required to direct the self-assembly into complex, device-oriented patterns that resemble integrated circuit layouts (cf. Section 2). If, however, the symmetry or length scale of the guiding pattern substantially deviates from the bulk morphology of the block copolymer material, the contact of the bulk material with a topographically or chemically structured surface results in the surface reconstruction of the copolymer structure. Since the free-energy differences between candidate copolymer structures are only a small fraction of the thermal energy scale k_BT per molecule, the geometry of and interaction with the guiding surface exert a great influence on the soft, copolymer material and, in contrast to crystalline atomistic solid, in which the reconstructed zone extends many nanometer away from the guiding pattern often propagating throughout the entire film thickness. An example of such a surface reconstruction at a patterned surface is depicted in Fig. 13, where a lamella-forming block copolymer is in contact with a guiding substrate that is comprised of a square array of spots that preferentially attract one component. The interplay between the lamellar bulk structure and the square guiding pattern gives rise to a complex, bicontinuous morphology in the thin film.

This example illustrates the challenge of designing guiding patterns for non-bulk structures, in particular, if one additionally requires the guiding pattern be sparse. Recently Hannon et al. have developed numerical optimization techniques to design guiding patterns composed of aperiodic arrays of nanoposts using a computational inverse design algorithm in conjunction with SCFT [54] and Qin et al. have devised a computational evolutionary strategy based on the time-dependent Ginzburg–Landau theory to design guiding patterns for irregular structure [55] and density multiplication [186]. In addition to these sophisticated numerical methods also physical guiding principles that underlie the surface reconstruction of periodic structures at patterned surfaces will contribute to a rational design of DSA patterns.

4. Process-directed self-assembly: tailoring the kinetics of structure formation

The discussion of the screening for suitable block copolymer materials and the precise control of film properties for the fabrication of desired structures have been based on equilibrium considerations, however, the kinetics of structure formation and, more generally, the processing of the material (e.g. by solvent treatment or thermal annealing protocols) are equally important [19,98,187–191].

For example, in Section 2.1, the similarity of thermodynamics and compression modulus of the triblock and corresponding diblock systems suggests that the significantly larger tolerance window from −13% to +55% in comparison with that of ±10% observed in AB diblock copolymers is not related to the equilibrium thermodynamics of the lamellar structure but rather a consequence of the kinetics. Indeed, the kinetics of structure formation in the triblock system is significantly slower than in diblocks. Additionally, simulations found that the systems assembled from two different starting configurations – a fingerprint morphology initially formed on the homogeneous neutral substrate and the disordered state mimicking the experimental disordered morphology before quenching – resulted in defect-free assembly only within the range $0.9\,L_0 \le L_S \le 1.2L_0$ in the former case but defect-free assembly was achieved for $0.9\,L_0 \le L_S \le 1.5L_0$ in

Please cite this article in press as: Li W, Müller M. Directed self-assembly of block copolymers by chemical or topographical guiding patterns: Optimizing molecular architecture, thin-film properties, and kinetics. Prog Polym Sci (2015), http://dx.doi.org/10.1016/j.progpolymsci.2015.10.008

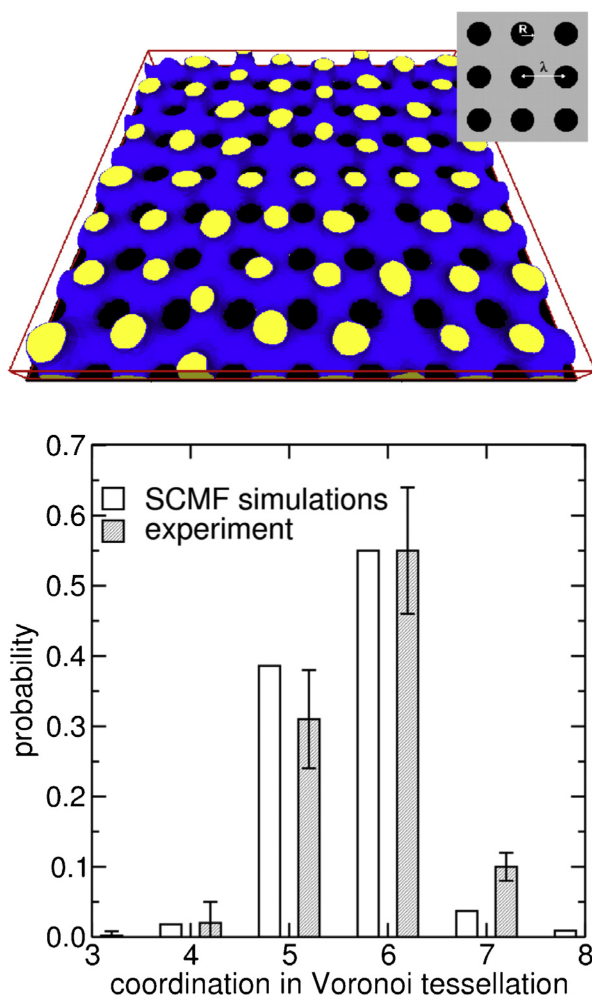

Fig. 13. (a) Surface reconstruction in a blend of lamella-forming PS-*b*-PMMA copolymer with corresponding homopolymers on a square array of spots (with radius $R = 0.2\,L_0$ and distance $\lambda = 1.12\,L_0$ cf. inset). In the simulation snapshot the PMMA domain has been removed and the internal PS-*b*-PMMA interface is shown in blue color. The bottom substrate is black and the PS-rich necks that emerge from the quadratically perforated layer at the substrate and reach the top surface are presented in yellow color. Ref. [184], Copyright 2006. Adapted with permission from the American Physical Society; (b) Probability distribution of the number of neighbors in a Voronoi analysis of the experimentally accessible structure at the top surface of the film. The shaded columns show experimental results whereas the data obtained by single-chain-in-mean-field simulations are presented by open bars. The "error bar" of the experimental results represents the variations that correspond to the size of the simulation cell. Ref. [185], Copyright 2006. Adapted with permission from John Wiley & Sons Inc. (For interpretation of the references to color in this figure legend, the reader is referred to the web version of this article.)

the latter case. Interestingly, the free energy of the defective structure obtained with the initial fingerprint configuration is even lower than that of the perfectly registered lamellar structure when $L_S > 1.2L_0$ indicating that the defect-free structures assembled from the disordered state are only metastable configurations [107].

In practical applications, thin films are routinely prepared by spin coating or solvent casting a mixture of copolymer and solvent onto a substrate. This process involves rapid (uncontrolled) solvent evaporation and, additionally, strong external fields (e.g. centrifugal forces or flow). As a result, it is very poorly understood. Qualitatively, the solvent evaporates and the concentration of the non-volatile polymer increases. In the simplest case, the co-solvent for the components of the block copolymer dilutes the repulsive interactions between unlike polymer blocks [192]. As the solvent evaporates, the thermodynamic driving force for microphase separation, quantified by the parameter χN, increases and, if the solvent concentration is sufficiently small, structure formation will begin. Importantly, the solvent also often acts as a plasticizer significantly speeding up the single-chain dynamics. These initial stages of microphase separation are critical because they have a significant influence on the morphologies during the further annealing steps and up to the final structures. Importantly, the final structures observed in experiments and simulations often do not correspond to complete thermal equilibrium but rather constitute metastable states in a complex, rugged free-energy landscape [95].

For instance, in order to remove defects that have formed during the initial stages of structure formation, the solvent-cast film is placed in an annealing chamber filled with solvent vapor. Tuning the evaporation rate by varying the vapor pressure one can control the orientation of morphologies [187,193–195]. Perpendicular or parallel cylinders have been experimentally observed in cylinder-forming block copolymer films using solvent annealing with controlled evaporation rates. However, no consistent picture of evaporation-induced ordering in block copolymer systems has been reached by experiments. Solvent evaporation from one-component polymer films has been studied by simulations and focused on the formation of a dense polymer layer (skin) at the free surface of the film [176,196] and the role of the glass transition [197]. Recently, Paradiso et al. have studied the ordering process of cylinder-forming block copolymer films during solvent evaporation using dynamic SCFT [190]. They find that the orientation of cylinders is controlled by the coupling effect of the evaporation rate and the effective segregation degree. Perpendicularly oriented structures tend to form under modest evaporation rates and relatively weak segregation strengths. Coarse-grained particle simulations have investigated the interplay between solvent-dependent incompatibility and single-chain dynamics on defect removal during solvent annealing [191]. This study also suggested that a two-stage solvent-annealing process might be advantageous for a controlled and reproducible structure formation because the first stage, at high solvent concentration, erases the structures in the as-cast film created by uncontrolled rapid solvent evaporation.

Temperature also has a pronounced influence on the kinetics of structure formation. Most notably, the single-chain dynamics critically depends on the distance from the glass transition temperature, T_g and increasing the temperature above T_g while simultaneously avoiding thermal degradation of polymer materials significantly accelerates the structure formation [198]. Such a thermal treatment can be conveniently incorporated into semiconductor

Please cite this article in press as: Li W, Müller M. Directed self-assembly of block copolymers by chemical or topographical guiding patterns: Optimizing molecular architecture, thin-film properties, and kinetics. Prog Polym Sci (2015), http://dx.doi.org/10.1016/j.progpolymsci.2015.10.008

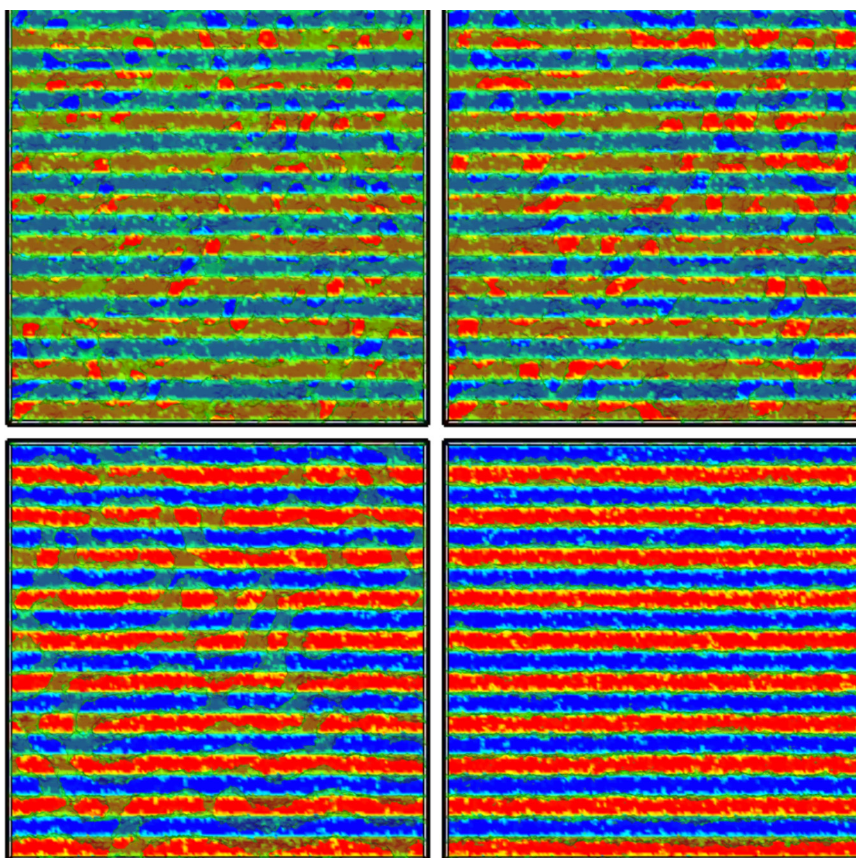

Fig. 14. Top-down images of structure evolution of a symmetric diblock copolymer on a L/S guiding pattern at $\chi N = 30$ obtained by simulations. The lateral system extensions are $L_y = L_z = 10\ L_0$ and the guiding pattern consists of strongly preferential, alternating A and B-attractive stripes of widths $W/L_0 = 1/2$. The different panels present snapshots at times $t/\tau = 0.11$, 0.34, 0.9, and 1.57 where τ denotes the time a polymer diffuses a distance of its size R_{e0} in the disordered state, $\chi N = 0$. Ref. [207], Copyright 2015. Reproduced with permission from the Institute of Physics.

industry production schemes. For some copolymer materials the Flory–Huggins parameter exhibits a sufficiently strong temperature dependence so that thermal annealing also significantly alters the thermodynamic conditions and a temperature increase may even bring the system into the disordered phase.

4.1. Surface-directed spinodal structure formation

Since the transition between the disordered state and ordered morphologies in pure diblock copolymers is only a very weak first-order transition in the bulk [199,200], the disordered state typically becomes unstable by lowering the temperature below the ODT temperature or reducing the solvent contents, and the spinodal kinetics of phase separation starts. On a non-patterned substrate, composition fluctuations with a wavelength comparable to the periodicity in the vicinity of the ODT spontaneously grow. At the end of this spinodal microphase separation, the composition attains its saturation values in the block copolymer domains but the structure is riddled with defects. In an intermediate stage of ordering, defects annihilate and larger grains with a specific orientation and low defect-density form. Grains of different orientations are separated by grain boundaries where defects are predominantly localized. In the final stage of ordering in the bulk or on a laterally uniform substrate, the grain structure coarsens via grain boundary motion. This universal mechanism has been studied by experiment, simulation, and theory [201–206].

In DSA, the film geometry – thickness or graphoepitaxial confinement – or the chemical guiding pattern in chemoepitaxy directs the spontaneous structure formation: (1) The guiding pattern determines the large-scale orientation and registration of the copolymer structure, thereby eliminating the last stage of the bulk ordering process—grain coarsening. (2) A judicious design of the guiding pattern directs the surface-directed spinodal structure formation. This initial stage is particularly important because the early morphology templates the structure of the later stages and can even lead to the formation of metastable structures instead of equilibrium structures. The importance of this surface-directed spinodal structure formation can be illustrated by the simple example of a lamella-forming copolymer on a guiding pattern that is comprised of lines and spaces (L/S) (cf. Fig. 14). Eventually, defect-free, registered, standing lamellae are formed [98], which correspond to the equilibrium structure.

Please cite this article in press as: Li W, Müller M. Directed self-assembly of block copolymers by chemical or topographical guiding patterns: Optimizing molecular architecture, thin-film properties, and kinetics. Prog Polym Sci (2015), http://dx.doi.org/10.1016/j.progpolymsci.2015.10.008

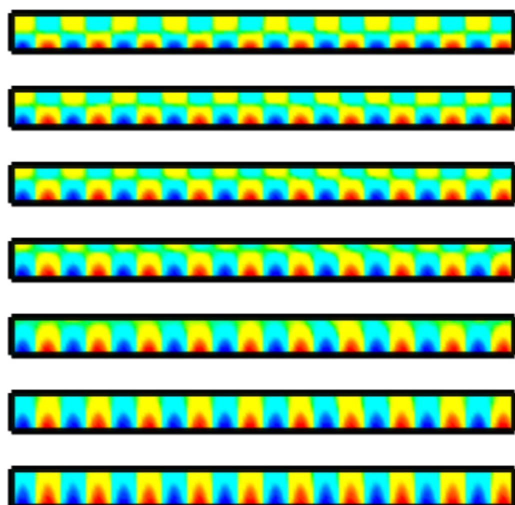

Fig. 15. Contour plots of the composition for the system in Fig. 14, obtained by averaging along the L/S pattern and over 10 independent simulations. The panels correspond to times $t/\tau = 0.11$, 0.22, 0.34, 0.45, 0.56, 0.67, and 0.9 from top to bottom. Ref. [207], Copyright 2015. Reproduced with permission from the Institute of Physics.

In the example presented in Figs. 14 and 15, the spacing of the bulk lamellar structure at $\chi N = 30$ perfectly matches the dimension of the guiding pattern on the substrate, and the film thickness $D = (3/4)L_0$ maximally frustrates lying lamellae. Nevertheless standing lamellae will not form immediately (cf. Fig. 14). Instead the surface-directed spinodal structure formation will give rise to a checkerboard pattern [208,209] that is clearly visible in the laterally averaged composition profiles depicted in Fig. 15. Within a fraction of the single-chain relaxation time τ, the copolymer structure replicates the guiding pattern at the bottom substrate of the film. On the top surface, in turn, a stripe structure also forms. This top stripe structure, however, has a weaker composition contrast and, importantly, it is shifted with respect to the guiding pattern by half a period. Thus, at the end of spinodal microphase separation, there are two lamellar grains – a registered one at the bottom substrate and a misaligned, shifted one at the top surface – that are separated by a horizontal grain boundary.

As the structure formation proceeds, this grain boundary moves upwards, i.e., the thickness of the aligned bottom grain grows and the top grain becomes thinner. As the top grain thins, the lamellar domains break up, giving rise to lines of dots (cf. Fig. 14 that are also observed in experiments [98]. Thus the DSA in a thin film on a patterned substrate does not proceed via lateral defect motion but via perpendicular grain-boundary motion.

This ordering process can be conceived as complete wetting. The two grains correspond to two coexisting phases – here, grains/phases only differ by their alignment – and the patterned substrate prefers the aligned grain. This preference is strong enough to induce a thick “wetting” layer of the preferred grain at the substrate.

Such a horizontal grain boundary can be stabilized in a thin film with two apposing patterned substrates. A particularly simple situation arises if the two patterned surfaces consists of the same stripe pattern that are rotated against each other by a twist angle α. In this case, a horizontal, twist grain boundary is formed. The morphology of lamella-forming block copolymers between two orthogonal, $\alpha = 90°$, chemically nano-patterned striped surfaces has been studied experimentally and such a set-up is instrumental to control the three-dimensional structure in a thin film [210].

The preference of the guiding pattern, ΛN, and the tension (free energy per area, γ_{gb}) of the grain boundary dictate whether the registered and aligned grain wets the substrate and the ordered structure will propagate from the substrate into the film. In a thin film with two apposing stripe patterns, the grain boundary will be delocalized in the middle of the film if both substrates prefer a thick aligned grain. If, however, the anchoring of the orientation and registration at the guiding substrate is only weak, the grain boundary will be localized either at the top or the bottom substrate, i.e., it is localized at the confining boundaries. These two states are illustrated in Fig. 16. The transition between these two states is the interface-localization–delocalization transition, and it is intimately related to the wetting transition [212,213]. Besides small film thickness corrections, it occurs when the surface free-energy difference of the aligned and misaligned grain $\Delta\gamma \sim \Lambda N \times k_BT\sqrt{\bar{N}}/R_{e0}^2$ is equal to the twist-angle-dependent grain-boundary tension γ_{gb} [211].

Altering the geometric characteristics – twist angle, film thickness and mismatch between the pattern period and the bulk lamellar spacing – one can exert exquisite control over the position of the grain boundary and thereby control the three-dimensional morphology. As illustrated in Fig. 15, it is important for DSA applications that the strength of the guiding pattern is strong enough to be in the delocalized state for the horizontal grain boundary, which forms in the course of surface-directed spinodal structure formation, be vertically pushed out of the film.

If the two-dimensional guiding pattern does not exactly match the bulk structure in its length scale or if the guiding pattern is sparse, localized defects will form in the course of structure formation. Thermodynamically, defects are local, metastable deviations from the perfectly ordered structure. At intermediate segregation, the excess free energy of defects ΔF_{defect}, is much larger than the thermal energy scale k_BT [95]. Thus these defects cannot be regarded as thermal equilibrium fluctuations around a perfectly ordered structure. This fact, $\Delta F > 20k_BT$, is important for DSA because it asserts that the equilibrium density of defects is vanishingly small. However, the observation of defects in experiments, in turn, indicates that they are formed in the initial course of structure formation.

Defects interact via the long-range distortions of structure, and these strain-mediated interactions [214] give rise to lateral motion of defects at intermediate stages of ordering. A prototypical class of defects are dislocations. For a more detailed discussion of defects and their relevance to DSA we refer the reader to a recent review [19]. Dislocations attract each other if their Burgers vectors point in opposite directions. If defects collide, they either annihilate or form a metastable tight dislocation pair. In the latter case, the structure formation is trapped in a long-lived metastable state. A rare thermal fluctuation is

Please cite this article in press as: Li W, Müller M. Directed self-assembly of block copolymers by chemical or topographical guiding patterns: Optimizing molecular architecture, thin-film properties, and kinetics. Prog Polym Sci (2015), http://dx.doi.org/10.1016/j.progpolymsci.2015.10.008

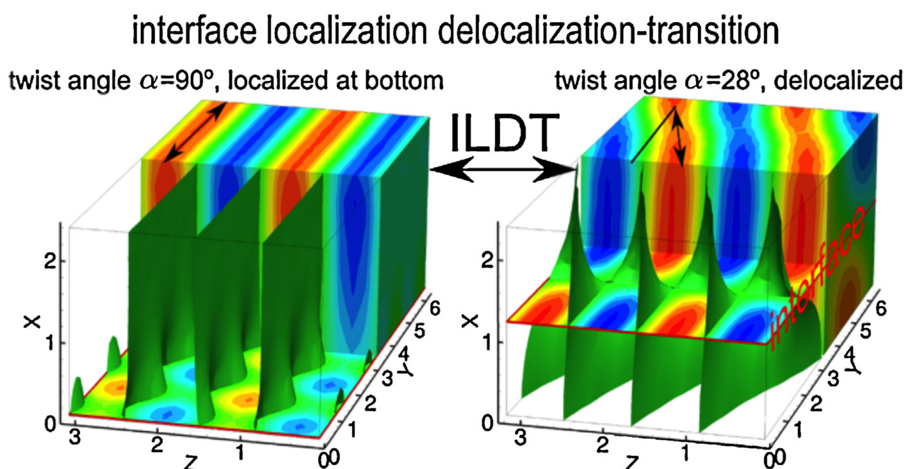

Fig. 16. Interface localization–delocalization transition of a horizontal twist grain boundary in a copolymer film between two stripe-patterned surfaces that are rotated against each other by a twist angle α. The images present contour plots of the time-averaged composition of the localized and delocalized state for a weakly preferential stripe pattern, $\Lambda N = 0.035$ and $\chi N = 20$, and two twist angles $\alpha = 90°$ ($m \geq 0$) and 28°, respectively. The positions of the twist grain boundary, $x \approx 0$ (localized state) and $x = D/2$ (delocalized state), are indicated by a plane. The green surfaces depicts the internal AB interfaces of the microphase-separated structure. Ref. [211], Copyright 2012. Reproduced with permission from the American Physical Society.

needed to escape this metastable structure. Since, for large incompatibilities, χN, or long polymer chains, $\bar{N}$, the overall collective free-energy scale in copolymer materials is much larger than k_BT, not only the excess free energy of a defect but also the free-energy barrier that characterizes its metastability is large, and the elimination of defects is protracted as evidenced by the long thermal annealing protocols employed in experiments, which exceed by far the single-chain relaxation time, τ.

Recent theoretical studies investigated the pathway along which defects are removed and revealed that the free energy barrier ΔF_b of defects decreases as the incompatibility χN decreases [96,133,215]. Interestingly, the barrier of removing a pair of dislocations in a lamellar stripe pattern vanishes at an incompatibility, χN_*, higher than the ODT, $\chi N_{ODT} = 10.5$ [96]. In the window of incompatibilities, $\chi N_{ODT} < \chi N < \chi N_*$, defects are not metastable and spontaneously transform into a defect-free stripe pattern. At χN_*, however, the excess free energy of a defect is much higher than k_BT, i.e., defects spontaneously annihilate and are not created by thermal fluctuations [96]. These thermodynamic conditions are ideally suited for DSA.

A detailed study of the mechanism of defect annihilation reveals that the pathway of removing a bound dislocation pair does proceed via the perpendicular motion of an interface that is the local analog of the perpendicular motion of the grain boundary during surface-directed spinodal structure formation (cf. Fig. 15) or the interface localization–delocalization transition (cf. Fig. 16). In accord with the wetting interpretation, the limiting incompatibility χN_* increases with the strength of the guiding pattern, thereby increasing the process window of DSA and accelerating the ordering process.

The detailed properties of defects are determined by a combination of thermodynamics and geometry – including commensurability between the pattern period and the domain spacing, contrast in interfacial tensions of the adjacent stripes of chemical patterns to distinct blocks, film thickness, and molecular architecture of copolymers. The relation between defect stability and wetting phenomena for bound dislocation pairs, however, suggests a rather universal mechanism and it is of interest to explore its applicability to other structures, e.g. triangular patterns of cylinders.

4.2. Nucleation induced defect-free domain patterns

Avoiding the occurrence of defects at the initial stage by tailoring the kinetic process provides an ideal strategy of fabricating defect-free patterns without a long period of defect annihilation. As alternative to surface-directed spinodal ordering, this basic idea can be realized via classic nucleation process that leads to epitaxial growth of single crystals from a metastable disordered phase (gas or liquid state), or of ordered structure of lower space symmetry from that of higher space symmetry. Specifically, the ordered phases of block copolymers exhibit similar characteristics as crystals, and therefore the concept of nucleation also holds for spatially modulated structures of block copolymers. For example, there is a first-order transition between the spherical phase and the disordered phase in the phase diagram of diblock copolymers [57]. Considering the effect of thermal fluctuations, even ODT between the symmetric lamellar phase and the disordered phase is first-order [200] albeit very weakly. When the disordered phase becomes metastable, the ordered spherical phase emerges via nucleation from the metastable disordered phase via a thermally activated process. Hashimoto et al. have observed the formation of isolated lamellar grains nucleated from the disordered state with a near symmetric PS-*b*-PI diblock copolymer [216], and they have also verified the nucleation process by the TDGL simulation based on the Swift–Hohenberg free energy functional [217].

The free energy barrier ΔF_b of forming a critical nucleus of the stable structure is determined by the bulk free

Please cite this article in press as: Li W, Müller M. Directed self-assembly of block copolymers by chemical or topographical guiding patterns: Optimizing molecular architecture, thin-film properties, and kinetics. Prog Polym Sci (2015), http://dx.doi.org/10.1016/j.progpolymsci.2015.10.008

energy difference and the interfacial energy between the stable crystal phase and the disordered phase. According to classical nucleation theory, the nucleation rate, defined by the probability of having one nucleation event in a unit volume per unit time, is proportional to the exponential term $\exp(-\Delta F_b/k_BT)$. Typically, nucleation events occur at a random position and at a random time. When ΔF_b is smaller than or comparable to thermal fluctuation energy k_BT, small fluctuations spontaneously grow and form ordered domains everywhere, i.e., structure formation proceeds via spinodal microphase-separation. In the absence of guiding patterns, structures formed via this spinodal mechanism often lack long-range order because thermal fluctuations at different positions simultaneously form multiple grains that do not have coherent locations and orientations. When the free energy barrier, ΔF_b, is increased to be significantly higher than k_BT, nucleation becomes a rare event, and the reduced nucleation rate leads to the formation of structures composed of a small number of spatially extended grains. Thus, the density of defects that are chiefly located at grain boundaries is significantly lowered. This rational argument suggests that we can reduce the defect density by decreasing the nucleation rate and thus forming fewer but larger grains. However, a lower nucleation rate, in turn, requires a longer incubation time that is required for a nucleation event to occur in a given sample. Therefore, structures on a macroscopic scale formed via spontaneous nucleation and growth are usually polycrystalline because it is unusually difficult and impractical to reduce the nucleation to a level where only a single nucleation event occurs in a macroscopic sample.

The nucleation in the absence of guiding patterns randomly occurs with a spatially uniform rate and is referred to as homogeneous nucleation. Homogeneous nucleation is hardly applicable to DSA because the time and location of nucleation events are random. Besides the activation of thermal fluctuation in homogeneous nucleation, external media, e.g. inclusions and specific boundaries, can be utilized to trigger nucleation events that are referred to as heterogeneous nucleation. In contrast to homogeneous nucleation, heterogeneous nucleation events can be controlled in time and space. Based on controllable heterogeneous nucleation, Xie et al. have proposed a new strategy to fabricate defect-free hexagonal cylinder patterns, and have demonstrated the feasibility of this strategy with sphere-forming block copolymer/homopolymer blends using TDGL simulations [97].

There are a number of critical conditions in the new strategy: (i) coexistence of stable ordered phase and metastable disordered phase, (ii) tunable nucleation rate that the stable ordered phase is nucleated from the metastable disordered phase, (iii) controllable heterogeneous nucleation leading to the formation of multiple ordered grains with unique orientation and commensurate locations. The intrinsic feature of the first-order transition between the ordered spherical phase and the disordered phase in compositionally asymmetric diblock copolymers ensures the coexistence of the stable spherical phase and the metastable disordered phase. As the metastability region of the disordered phase with respect to the temperature for a specific copolymer is limited in the phase diagram of neat diblock copolymers [218], the AB diblock copolymer/C homopolymer blend, in which A block is minority and C homopolymer is B-selective, is used instead. In the binary blends, the composition of C homopolymer $\bar{\phi}_C$ is varied to regulate the stability of the disordered phase and thus to control the nucleation rate (Fig. 17). In 2D simulations, spherical and cylindrical domains are indistinguishable. In fact, perpendicular cylinders can be formed in thin films of sphere-forming block copolymers when the two surfaces are neutral and the film thickness is significantly smaller than the domain spacing [219,220]. As decreasing the composition of C, the nucleation rate related to the number of grains formed at the initial stage decreases, and concomitantly the incubation time increases. Accordingly, the order of cylinder patterns is gradually improved as decreasing the composition of C homopolymers. Note that, although there is only single nucleated grain in the entire sample when $\bar{\phi}_C = 0.03$, it is not guaranteed that one, and only one, nucleation event will occur in a much larger sample with a macroscopic size. Nevertheless, it is unfeasible to obtain a single nucleated grain that grows up to occupy the entire sample and thus to form defect-free domain patterns.

Sparsely periodic spot arrays of chemical patterns on substrates are able to act as the nucleation agents simultaneously inducing heterogeneous nucleation event on each nucleus. Fig. 18(a) indicates that each nucleation agent, formed by a potential well attracting to the minority block, induces a cylinder of the minority blocks at the location of the nucleation agent as soon as the potential is switched on [97]. Each induced cylinder can then act as the core of the nucleus, thus eliminating the incubation time and successfully activating the nucleation growth. During the growth course, there is no spontaneous nucleation event occurred indicating that the nucleation rate is low enough to suppress homogeneous nucleation. Domain grains nucleated from the periodic array of potential spots exhibit random orientations due to the isotropic nature of the circularly symmetric nucleation agent, and therefore they still form polycrystalline domain structures at the end of the growth process because of their mismatched orientations (Fig. 18(b)). In order to take advantage of the full potential of multiple nucleation agents, it is essential to design an anisotropic unit of nucleation agent that is capable of controlling both the position and orientation of an ordered domain grain. As a demonstration, the simple double-spot potential on a sparsely periodic array has the capability to induce one nucleus at a given position and with a given orientation (Fig. 18(c)). Therefore the array of induced domain grains are coherent in that their positions are commensurate with the ordered block copolymer phase and their orientations are uniform. The growth of these coherent grains leads to the formation of a defect-free pattern. Here the period of the nucleation-agent array can be as large as tens of times of the domain spacing, exhibiting a density multiplication much higher than the reported limit, 25 [16,61]. Furthermore, it has been demonstrated that the six corners of a hexagonal well are able to act as nucleation agents triggering nucleation events whose growth leads to perfectly ordered hexagonal patterns in the entire well [221].

Please cite this article in press as: Li W, Müller M. Directed self-assembly of block copolymers by chemical or topographical guiding patterns: Optimizing molecular architecture, thin-film properties, and kinetics. Prog Polym Sci (2015), http://dx.doi.org/10.1016/j.progpolymsci.2015.10.008

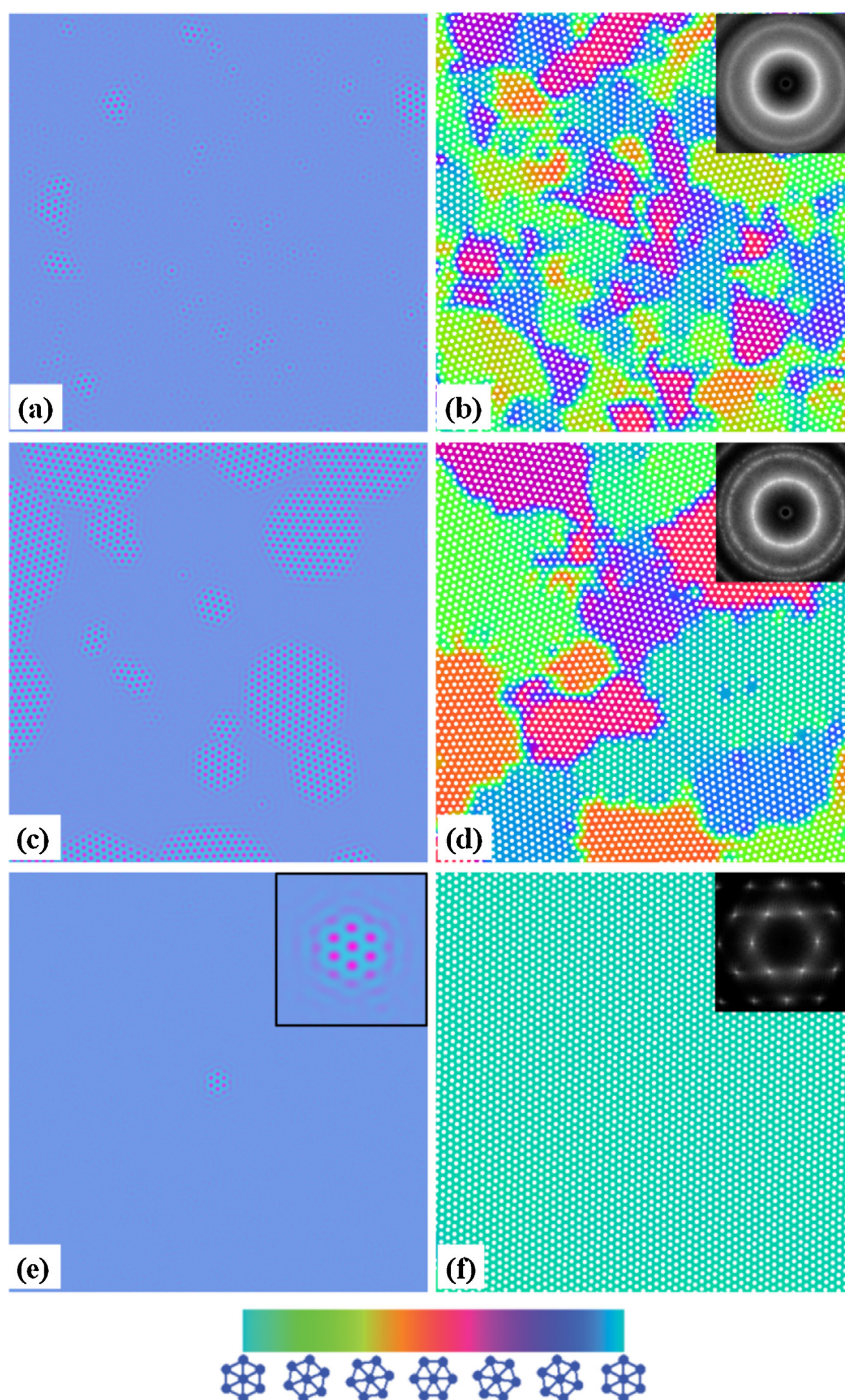

Fig. 17. Density configurations of A blocks for various homopolymer compositions of $\bar{\phi}_C$ at the initial nucleating stage (left column) and at the late stage when the nucleation growth just ends (right column), respectively. (a) t = 10,000 and (b) t = 20,000 for $\bar{\phi}_C = 0.050$; (c) t = 30,000 and (d) t = 90,000 for $\bar{\phi}_C = 0.040$; (e) t = 185,000 and (f) t = 340,000 for $\bar{\phi}_C = 0.030$. For the figures of right column, their orientational order is indicated by the bottom color spectrum, and their insets give the corresponding Fourier transformations. Ref. [97], Copyright 2013. Reproduced from the Royal Society of Chemistry. (For interpretation of the references to color in this figure legend, the reader is referred to the web version of this article.)

The patterning approach via heterogeneous nucleation induced by multiple nucleation agents is versatile due to a vast classical nucleation knowledge. For instance, a multitude of types of nucleation agents can be chosen, such as sidewall surfaces and geometrical corners in topographical patterns. Furthermore, the idea of fabricating defect-free patterns on large scale via nucleation process is not limited to the case of a stable ordered phase

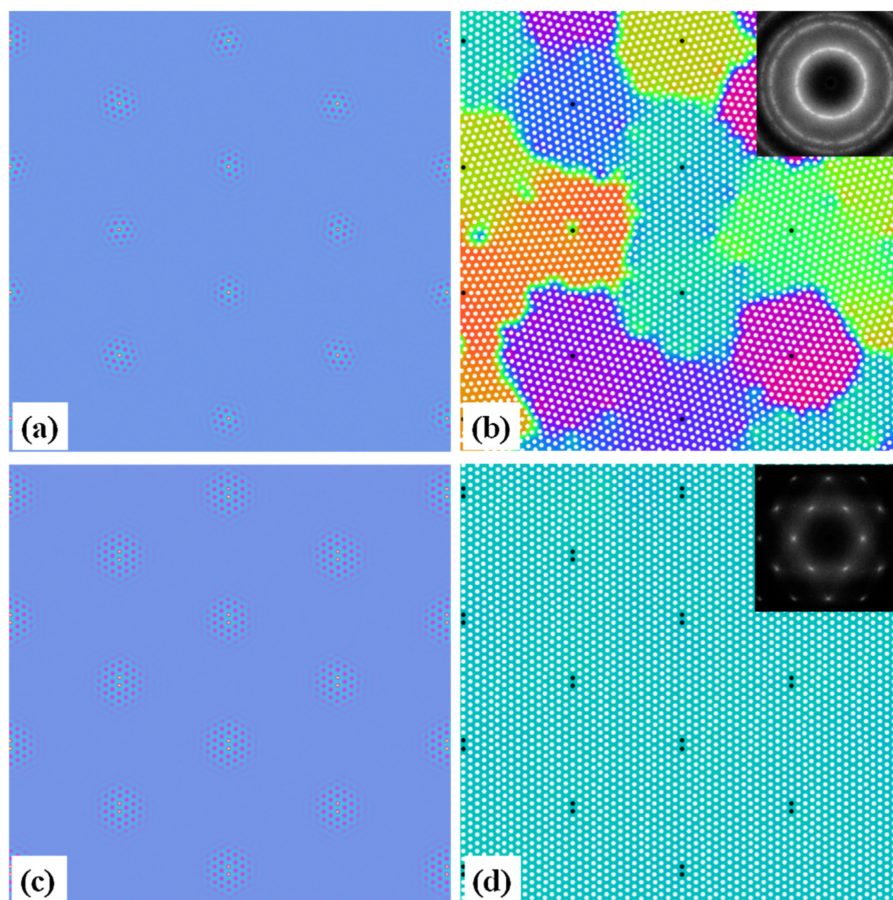

Fig. 18. Snapshots of density configurations of morphologies formed by the heterogeneous nucleation process that proceeds via the induced nucleation of the stable ordered cylinder phase from the metastable disordered state by the sparsely period array of potential spots. The concentration of homopolymers is set as $\bar{\phi}_C = 0.03$ leading to a reasonable low nucleation rate that is able to suppress homogeneous spontaneous nucleation events during the growth period of the induced nucleation grains. (a) and (b) The unit of nucleation agent is acted by the circularly symmetric spot inducing nucleated domains with random orientations and hence still resulting in a polycrystalline morphology. (c) and (d) The unit of nucleation agent is replaced with double spots with a separation equal to the domain spacing of the bulk cylinder phase. Coherent nucleation grains are induced giving rise to defect-free cylinder patterns. Potential spots are highlighted by black filled circles. Ref. [97], Copyright 2013. Reproduced from the Royal Society of Chemistry.

nucleated from a metastable disordered phase, while it can be extended to more general situations, i.e. a stable ordered phase nucleated from another metastable ordered phase. In experiments, Sota et al. have prepared large-scale ordered morphologies of bcc spheres via nucleating sphere domains from highly aligned hexagonal cylinders, and the nucleation process is triggered by a temperature jump [222]. Therefore the introduction of heterogeneous nucleation concept might open a new perspective for the patterning technique of DSA.

5. Perspectives

Directed self-assembly of block copolymers (DSA) on patterned substrates has attracted abiding theoretical and experimental interest for its perspective as one of the most promising patterning techniques at the nanoscale. As a consequence, great efforts have been directed to systematically develop experimental protocols as well as an understanding of the underlying physics. Using the model diblock copolymer, PS-*b*-PMMA, previous studies demonstrated the successful fabrication of defect-free patterns of lines and spaces or triangular arrangement of cylinders via chemoepitaxy or graphoepitaxy, and even irregular device-oriented structures have been replicated.

To address requirements for potential applications in nanotechnology, efforts are directed to fabricate nanostructure with smaller characteristic dimension or more complex structures. In this review we have discussed three aspects that may contribute to the development of nano patterning techniques: (i) optimizing the equilibrium thermodynamic properties of DSA materials by selecting the molecular architecture like ABA triblock copolymers, to ABC linear or star triblock terpolymers, and even to more complex multiblock copolymers (ii) controlling the film properties such as film thickness as well as geometry of guiding pattern and surface interactions, and (iii) tailoring the kinetics of structure formation.

Additional open questions include *inter alia*:

(i) Further miniaturization of structures implies that guiding patterns will be sparse or will have larger

Please cite this article in press as: Li W, Müller M. Directed self-assembly of block copolymers by chemical or topographical guiding patterns: Optimizing molecular architecture, thin-film properties, and kinetics. Prog Polym Sci (2015), http://dx.doi.org/10.1016/j.progpolymsci.2015.10.008

dimensions than the structure formed by the copolymer (density multiplication). In this case the guiding pattern merely directs the large scale orientation and registration. For the experimental fabrication of defect-free stripe pattern by lamella-forming block copolymers on chemical patterns the highest density multiplication is 4 [45], and it does not exceed 25 for the fabrication of hexagonal cylinder patterns via graphoepitaxy [16]. Additional progress, however, is required to fully exploit this concept and to achieve larger factors of density multiplication.

(ii) Metastable structures are typically formed in the course of block copolymer self-assembly. The single-chain dynamics of macromolecular materials and the large free-energy scale of systems with a large degree of polymerization imparts a protracted lifetime onto these metastable state such that they can be easily trapped and stabilized. Tailoring the kinetics of structure formation by guiding patterns on the film substrate or temporal variations of the thermodynamic process conditions (e.g. temperature or solvent pressure) offers ample opportunities to direct the kinetics of microphase separation, which have only recently been exploited.

(iii) In the practical application of fabricating integrated circuit layouts, different geometric structure are usually demanded, e.g. structures that consists of domains of dot arrays and lines-and-space patterns. The characteristics of block copolymer materials dictates that microphase separated structures are dense, periodic structures whose domain dimension and geometry is on the same order of magnitude as the molecular dimensions (e.g. end-to-end distance, R_{e0}). Hierarchical structure formation comprised of controlled macrophase separation of a macromolecular blends guided by substrate patterns and subsequent microphase separation might offer an approach for fabricating structures with large areas of different small-scale structures.

Acknowledgments

It is great pleasure to thank K.Ch. Daoulas, E.W. Edwards, J.J. de Pablo, S.X. Ji, P.F. Nealey, A.C. Shi, R. Shenhar, M.P. Stoykovich, D.W. Sun, and U. Welling for stimulating discussions and fruitful collaboration. This work was supported by the European Union FP7 under grant agreement 619793 CoLiSA.MMP (Computational Lithography for Directed Self-Assembly: Materials, Models, and Processes). W. L. thanks the National Natural Science Foundation of China (NSFC) (Grants nos. 21322407 and 21574026) for additional financial support. We thank the GWDG Göttingen, the HLRN Berlin/Hannover, and the Jülich Supercomputing Centre for ample computing time.

References

[1] Bates FS, Fredrickson GH. Block copolymer thermodynamics—theory and experiment. Ann Rev Phys Chem 1990;41:525–57.
[2] Park C, Yoon J, Thomas EL. Enabling nanotechnology with self-assembled block copolymer patterns. Polymer 2003;44:6725–60.
[3] Segalman RA. Patterning with block copolymer thin films. Mater Sci Eng R-Rep 2005;48:191–226.
[4] Bates FS, Hillmyer MA, Lodge TP, Bates CM, Delaney KT, Fredrickson GH. Multiblock polymers: Panacea or pandoras's box? Science 2012;336:434–40.
[5] Darling SB. Directing the self-assembly of block copolymers. Prog Polym Sci 2007;32:1152–204.
[6] Hamley IW. Ordering in thin films of block copolymers: Fundamentals to potential applications. Prog Polym Sci 2009;34:1161–210.
[7] Kim HC, Park SM, Hinsberg WD. Block copolymer based n anostructures: materials, processes, and applications to electronics. Chem Rev 2010;110:146–77.
[8] Herr DJC. Directed block copolymer self-assembly for nanoelectronics fabrication. J Mater Res 2011;26:122–39.
[9] Koo K, Ahn H, Kim SW, Ryu DY, Russell TP. Directed self-assembly of block copolymers in the extreme: guiding microdomains from the small to the large. Soft Matter 2013;9:9059–71.
[10] Marencic AP, Adamson DH, Chaikin PM, Register RA. Shear alignment and realignment of sphere-forming and cylinder-forming block copolymer thin films. Phys Rev E: Stat Nonlinear Soft Matter Phys 2010;81:011503/1–11503.
[11] Hu H, Gopinadhan M, Osuji CO. Directed self-assembly of block copolymers: a tutorial review of strategies for enabling nanotechnology with soft matter. Soft Matter 2014;10:3867–89.
[12] Luo M, Epps III TH. Directed block copolymer thin film self-assembled: emerging trends in nanopattern fabrication. Macromolecules 2013;46:7567–79.
[13] Bates CM, Maher MJ, Janes DW, Ellison CJ, Willson CG. Block copolymer lithography. Macromolecules 2014;47:2–12.
[14] Kim SO, Solak HH, Stoykovich MP, Ferrier NJ, de Pablo JJ, Nealey PF. Epitaxial self-assembly of block copolymers on lithographically defined nanopatterned substrates. Nature 2003;424:411–4.
[15] Stoykovich MP, Müller M, Kim SO, Solak HH, Edwards EW, de pablo JJ, Nealey PF. Directed assembly of block copolymer blends into nonregular device-oriented structures. Science 2005;308:1442–6.
[16] Bita I, Yang JKW, Jung YS, Ross CA, Thomas EL, Berggren KK. Graphoepitaxy of self-assembled block copolymers on two-dimensional periodic patterned templates. Science 2008;321:939–43.
[17] Ruiz R, Kang HM, Detcheverry FA, Dobisz E, Kercher DS, Albrecht TR, de pablo JJ, Nealey PF. Density multiplication and improved lithography by directed block copolymer assembly. Science 2008;321:936–9.
[18] Chang JB, Choi HK, Hannon AF, Alexander-Katz A, Ross CA, Berggren KK. Design rules for self-assembled block copolymer patterns using tiled templates. Nat Commun 2014;5:3305/1–3305.
[19] Li WH, Müller M. Defects in the self-assembly of block copolymers and their relavance for directed self-assembly. Annu Rev Chem Biomol Eng 2015;6:187–216.
[20] Ruiz R, Sandstrom RL, Black CT. Induced orientational order in symmetric diblock copolymer thin films. Adv Mater 2007;19:587–91.
[21] Campbell IP, Lau GJ, Feaver JL, Stoykovich MP. Network connectivity and long-range continuity of lamellar morphologies in block copolymer thin films. Macromolecules 2012;45:1587–94.
[22] Campbell IP, He C, Stoykovich MP. Topologically distinct lamellar block copolymer morphologies formed by solvent and thermal annealing. ACS Macro Lett 2013;2:918–23.
[23] Campbell IP, Hirokawa S, Stoykovich MP. Processing approaches for the defect engineering of lamellar-forming block copolymers in thin films. Macromolecules 2013;46:9599–608.
[24] Chen ZR, Kornfield JA, Smith SD, Grothaus JT, Satkowski MM. Pathways to macroscale order in nanostructured block copolymers. Science 1997;277:1248–53.
[25] Ren SR, Hamley IW, Teixeira PIC, Olmsted PD. Cell dynamics simulations of shear-induced alignment and defect annihilation in stripe patterns formed by block copolymers. Phys Rev E: Stat Nonlinear Soft Matter Phys 2001;63:041503/1–41503.
[26] Angelescu DE, Waller JH, Adamson DH, Deshpande P, Chou SY, Register RA, Chaikin PM. Macroscopic orientation of block copolymer cylinders in single-layer films by shearing. Adv Mater 2004;16:1736–40.
[27] Angelescu DE, Waller JH, Register RA, Chaikin PM. Shear-induced alignment in thin films of spherical nanodomains. Adv Mater 2005;17:1878–81.
[28] Luo KF, Yang YL. Orientational phase transitions in hexagonal cylinder phase and kinetic pathways of lamellar phase to hexagonal phase transition of asymmetric diblock copolymers under steady shear flow. Polymer 2004;19:6745–51.

Please cite this article in press as: Li W, Müller M. Directed self-assembly of block copolymers by chemical or topographical guiding patterns: Optimizing molecular architecture, thin-film properties, and kinetics. Prog Polym Sci (2015), http://dx.doi.org/10.1016/j.progpolymsci.2015.10.008

[29] Arya G, Rottler J, Panagiotopoulos AZ, Srolovitz DJ, Chaikin PM. Shear ordering in thin films of spherical block copolymer. Langmuir 2005;21:11518–27.
[30] Wu MW, Register RA, Chaikin PM. Shear alignment of sphere-morphology block copolymer thin films with viscous fluid flow. Phys Rev E: Stat Nonlinear Soft Matter Phys 2006;74:040801/1–40801.
[31] Rottler J, Srolovitz DJ. Mechanism of shear induced alignment in bilayer thin films of spherical particles. Phys Rev Lett 2007;98:175503/1–175503.
[32] Marencic AP, Wu MW, Register RA, Chaikin PM. Orientational order in sphere-forming block copolymer thin films aligned under shear. Macromolecules 2007;40:7299–305.
[33] Pujari S, Keaton MA, Chaikin PM, Register RA. Alignment of perpendicular lamellae in block copolymer thin films by shearing. Soft Matter 2012;8:5358–63.
[34] Amundson K, Helfand E, Quan X, Hudson SD, Smith SD. Alignment of lamellar block copolymer microstructure in an electric field. 2. Mechanisms of alignment. Macromolecules 1994;27:6559–70.
[35] Morkved TL, Lu M, Urbas AM, Ehrichs EE, Jaeger HM, Mansky P, Russell TP. Local control of microdomain orientation in diblock copolymer thin films with electric fields. Science 1996;273:931–3.
[36] Thurn-Albrecht T, DeRouchey J, Russell TP, Jaeger HM. Overcoming interfacial interactions with electric fields. Macromolecules 2000;33:3250–3.
[37] Böker A, Elbs H, Hänsel H, Knoll A, Ludwigs S, Zettl H, Urban V, Abetz V, Müller AHE, Krausch G. Microscopic mechanisms of electric-field-induced alignment of block copolymer microdomains. Phys Rev Lett 2002;89:135502/1–135502.
[38] Zvelindovsky AV, Sevink GJA. Comment on "microscopic mechanisms of electric-field-induced alignment of block copolymer microdomains". Phys Rev Lett 2003;90:049601/1.
[39] Olszowka V, Kuntermann V, Böker A. Control of orientational order in block copolymer thin films by electric fields: a combinatorial approach. Macromolecules 2008;41:5515–8.
[40] Pinna M, Schreier L, Zvelindovsky AV. Mechanisms of electric-field-induced alignment of block copolymer lamellae. Soft Matter 2009;5:970–3.
[41] Zhang JL, Yu XH, Yang P, Peng J, Luo CX, Huang WH, Han YC. Microphase separation of block copolymer thin films. Macromol Rapid Comm 2010;31:591–608.
[42] Liedel C, Hund M, Olszowka V, Böker A. On the alignment of a cylindrical block copolymer: a time-resolved and 3-dimensional SFM study. Soft Matter 2012;8:995–1002.
[43] Ruppel M, Pester CW, Langner KM, Sevink JA, Schoberth HG, Schmidt K, Urban VS, Mays JW, Böker A. Electric field induced selective disordering in lamellar block copolymers. ACS Nano 2013;7:3854–67.
[44] Welling U, Müller M, Shalev H, Tsori Y. Block copolymer ordering in cylindrical capacitors. Macromolecules 2014;47:1850–64.
[45] Cheng JY, Rettner CT, Sanders DP, Kim HC, Hinsberg WD. Dense self-assembly on sparse chemical patterns: rectifying and multiplying lithographic patterns using block copolymers. Adv Mater 2008;20:3155–8.
[46] Liu CC, Ramirez-Hernandez A, Han E, Craig GSW, Tada Y, Yoshida H, Kang HM, Ji SX, Gopalan P, de Pablo JJ, Nealey PF. Chemical patterns for directed self-assembly of lamellae-forming block copolymers with density multiplication of features. Macromolecules 2013;46:1415–24.
[47] Segalman RA, Yokoyama H, Kramer EJ. Graphoepitaxy of spherical domain block copolymer films. Adv Mater 2001;13:1152–5.
[48] Cheng JY, Mayes AM, Ross CA. Nanostructure engineering by templated self-assembly of block copolymers. Nat Mater 2004;3:823–8.
[49] Tavakkoli AKG, Gotrik KW, Hannon AF, Alexander-Katz A, Ross CA, Berggren KK. Templating three-dimensional self-assembled structures in bilayer block copolymer films. Science 2012;336:1294–8.
[50] Stoykovich MP, Kang H, Daoulas KC, Liu G, Liu CC, de Pablo JJ, Müller M, Nealey PF. Directed self-assembly of block copolymers for nanolithography: fabrication of isolated features and essential integrated circuit geometries. ACS Nano 2007;1:168–75.
[51] Yang JKW, Jung YS, Chang JB, Mickiewicz RA, Alexander-Katz A, Ross CA, Berggren KK. Complex self-assembled patterns using sparse commensurate templates with locally varying motifs. Nat Nanotechnol 2010;5:256–60.
[52] Mickiewicz RA, Yang JKW, Hannon AF, Jung YS, Alexander-Katz A, Berggren KK, Ross CA. Enhancing the potential of block copolymer lithography with polymer self-consistent field theory simulations. Macromolecules 2010;43:8290–5.
[53] Chang JB, Son JG, Hannon AF, Alexander-Katz A, Ross CA, Berggren KK. Aligned sub-10-nm block copolymer patterns templated by post arrays. ACS Nano 2012;6:2071–7.
[54] Hannon AF, Gotrik KW, Ross CA, Alexander-Katz A. Inverse design of topographical templates for directed self-assembly of block copolymers. ACS Macro Lett 2013;2:251–5.
[55] Qin J, Khaira GS, Su YR, Garner GP, Miskin M, Jaeger HM, de Pablo JJ. Evolutionary pattern design for copolymer directed self-assembly. Soft Matter 2013;9:11467–72.
[56] Zhang LS, Wang LQ, Lin JP. Harnessing anisotropic nanoposts to enhance long-range orientation order of directed self-assembly nanostructures via large cell simulations. ACS Macro Lett 2014;3:712–6.
[57] Matsen MW, Schick M. Stable and unstable phases of a diblock copolymer melt. Phys Rev Lett 1994;72:2660–3.
[58] Matsen MW. The standard Gausian model for block copolymer melts. J Phys Condens Matter 2002;14:R21–47.
[59] Tyler CA, Morse DC. Orthorhombic Fddd network in triblock and diblock copolymer melts. Phys Rev Lett 2005;94:208302.
[60] Tada Y, Akasaka S, Takenaka M, Yoshida H, Ruiz R, Dobisz E, Hasegawa H. Nine-fold density muliplication of hcp lattice pattern by directed self-assembly of block copolymer. Polymer 2009;50:4250–6.
[61] Li WH, Qiu F, Yang YL, Shi AC. Ordering dynamics of directed self-assembly of block copolymers in periodic two-dimensional fields. Macromolecules 2010;43:1644–50.
[62] Li WH, Xie N, Qiu F, Yang YL, Shi AC. Ordering kinetics of block copolymers directed by periodic two-dimensional rectangular fields. J Chem Phys 2011;134:144901/1–144901.
[63] Park SM, Craig GSW, La YH, Solak HH, Nealey PF. Square arrays of vertical cylinders of PS-*b*-PMMA on chemically nanopatterned surfaces. Macromolecules 2007;40:5084–94.
[64] Hur SM, Garcia-Cervera CJ, Kramer EJ, Fredrickson GH. SCFT simulations of thin film blends of block copolymer and homopolymer laterally confined in a square well. Macromolecules 2009;42:5861–72.
[65] Xu J, Russell TP, Ocko BM, Checco A. Block copolymer self-assembly in chemically patterned squares. Soft Matter 2011;7:3915–9.
[66] Mogi Y, Kotsuji H, Kaneko Y, Mori K, Matsushita Y, Noda I. Preparation and morphology of triblock copolymers of the ABC type. Macromolecules 1992;25:5408–11.
[67] Matsen MW. Gyroid versus double-diamond in ABC triblock copolymer melts. J Chem Phys 1998;108:785–96.
[68] Daoulas KC, Cavallo A, Shenhar R, Müller M. Directed assembly of supramolecular copolymers in thin films: thermodynamic and kinetic advantages. Phys Rev Lett 2010;105:108301/1–108301.
[69] Drolet F, Fredrickson GH. Combinatorial screening of complex block copolymer assembly with self-consistent field theory. Phys Rev Lett 1999;83:4317–20.
[70] Fredrickson GH. The equilibrium theory of inhomogeneous polymers. Oxford: Clarendon Press; 2006. p. 203–81.
[71] Rasmussen KØ, Kalosakas G. Improved numerical algorithm for exploring block copolymer mesophases. J Polym Sci, B: Polym Phys 2002;40:1777–83.
[72] Tyler CA, Qin J, Bates FS, Morse DC. SCFT study of nonfrustrated ABC triblock copolymer melts. Macromolecules 2007;40:4654–68.
[73] Li WH, Qiu F, Shi AC. Emergence and stability of helical superstructures in ABC triblock copolymers. Macromolecules 2012;45:503–9.
[74] Liu MJ, Li WH, Qiu F, Shi AC. Theoretical study of phase behavior of frustrated ABC linear triblock copolymers. Macromolecules 2012;45:9522–30.
[75] Mogi Y, Nomura M, Kotsuji H, Ohnishi K, Matsushita Y, Noda I. Superlattice structures in morphologies of the ABC triblock copolymers. Macromolecules 1994;27:6755–60.
[76] Stadler R, Auschra C, Beckmann J, Krappe U, Voigtmartin I, Leibler L. Morphology and thermodynamics of symmetrical poly(A-*block*-B-*block*-C) triblock copolymers. Macromolecules 1995;28:3080–97.
[77] Breiner U, Krappe U, Thomas EL, Stadler R. Structural characterization of the "knitting pattern" in Polystyrene-*block*-poly(ethylene-*co*-butylene)-*block*-poly(methylmethacrylate) triblock copolymers. Macromolecules 1998;31:135–41.
[78] Elbs H, Abetz V, Hadziioannou G, Drummer C, Krausch G. Antiferromagnetic ordering in a helical triblock copolymer mesostructure. Macromolecules 2001;34:7917–9.
[79] Elbs H, Drummer C, Abetz V, Krausch G. Thin film morphologies of ABC triblock copolymers prepared from solution. Macromolecules 2002;35:5570–7.

Please cite this article in press as: Li W, Müller M. Directed self-assembly of block copolymers by chemical or topographical guiding patterns: Optimizing molecular architecture, thin-film properties, and kinetics. Prog Polym Sci (2015), http://dx.doi.org/10.1016/j.progpolymsci.2015.10.008

[80] Nagpal U, Detcheverry FA, Nealey PF, de Pablo JJ. Morphologies of linear triblock copolymers from Monte Carlo simulations. Macromolecules 2011;44:5490–7.
[81] Takano A, Wada S, Sato S, Araki T, Hirahara K, Kazama T, Kawahara S, Isono Y, Ohno A, Tanaka N, Matsushita Y. Observation of cylinder-based microphase-separated structures from ABC star-shaped terpolymers investigated by electron computerized tomography. Macromolecules 2004;37:9941–6.
[82] Hayashida K, Kawashima W, Takano A, Shinohara Y, Amemiya Y, Nozue Y, Matsushita Y. Archimedean tiling patterns of ABC star-shaped terpolymers studied by microbeam small-angle X-ray scattering. Macromolecules 2006;39:4869–72.
[83] Li WH, Xu YC, Zhang GJ, Qiu F, Yang YL, Shi AC. Real-space self-consistent mean-field theory study of ABC star triblock copolymers. J Chem Phys 2010;133:064904/1–64904.
[84] Zhang GJ, Qiu F, Zhang HD, Yang YL, Shi AC. SCFT study of tiling patterns in ABC star terpolymers. Macromolecules 2010;43:2981–9.
[85] Xie N, Liu MJ, Deng HL, Li WH, Qiu F, Shi AC. Macromolecular metallurgy of binary mesocrystals via designed multiblock terpolymers. J Am Chem Soc 2014;136:2974–7.
[86] Bates FS, Maurer WW, Lipic PM, Hillmyer MA, Almdal K, Mortensen K, Fredrickson GH, Lodge TP. Polymeric bicontinuous microemulsions. Phys Rev Lett 1997;79:849–52.
[87] Janert PK, Schick M. Phase behavior of ternary homopolymer/diblock blends: microphase unbinding in the symmetric system. Macromolecules 1997;30:3916–20.
[88] Janert PK, Schick M. Phase behavior of binary homopolymer/diblock blends: temperature and chain length dependence. Macromolecules 1998;31:1109–13.
[89] Matsen MW. Phase behavior of block copolymer/homopolymer blends. Macromolecules 1995;28:5765–73.
[90] Müller M, Schick M. Bulk and interfacial thermodynamics of a symmetric, ternary homopolymer copolymer mixture: a Monte Carlo study. J Chem Phys 1996;105:8885–901.
[91] Wang Q, Nealey PF, de Pablo JJ. Monte Carlo simulations of asymmetric diblock copolymer thin films confined between two homogeneous surfaces. Macromolecules 2001;34:3458–70.
[92] Stein GE, Cochran EW, Katsov K, Fredrickson GH, Kramer EJ, Li X, Wang J. Symmetry breaking of in-plane order in confined copolymer mesophases. Phys Rev Lett 2007;98:158302/1–158302.
[93] Li WH, Liu MJ, Qiu F, Shi AC. Phase diagram of diblock copolymers confined in thin films. J Phys Chem B 2013;117:5280–8.
[94] Meng D, Wang Q. Complex morphologies in thin films of symmetric diblock copolymers as stable and unstable phases. Soft Matter 2010;6:5891–906.
[95] Nagpal U, Müller M, Nealey PF, de Pablo JJ. Free energy of defects in ordered assemblies of block copolymer domains. ACS Macro Lett 2012;1:418–22.
[96] Li WH, Nealey PF, de Pablo JJ, Müller M. Defect removal in the course of directed self-assembly is facilitated in the vicinity of the order–disorder transition. Phys Rev Lett 2014;113:168301/1–168301.
[97] Xie N, Li WH, Qiu F, Shi AC. New strategy of nanolithography via controlled block copolymer self-assembly. Soft Matter 2013;9:536–42.
[98] Edwards EW, Stoykovich MP, Müller M, Solak HH, de Pablo JJ, Nealey FF. Mechanism and kinetics of ordering in diblock copolymer thin films on chemically nanopatterned substrates. J Polym Sci, B: Polym Phys 2005;43:3444–59.
[99] Müller M, Sun DW. Directing the self-assembly of block copolymers into a metastable complex network phase via a deep and rapid quench. Phys Rev Lett 2013;111:267801/1–267801.
[100] Yang XM, Xiao SG, Liu C, Pelhos K, Minor K. Nanoscopic templates using self-assembled cylindrical diblock copolymers for patterned media. J Vac Sci Technol B 2004;22:3331–4.
[101] Edwards EW, Müller M, Stoykovich MP, Solak HH, de Pablo JJ, Nealey FF. Dimensions and shapes of block copolymer domains assembled on lithographically defined chemically patterned substrates. Macromolecules 2007;40:90–6.
[102] Tada Y, Akasaka S, Yoshida H, Hasegawa H, Dobisz E, Kercher D, Takenaka M. Directed self-assembly of diblock copolymer thin films on chemically-patterned substrates for defect-free nanopatterning. Macromolecules 2008;41:9267–76.
[103] Yang XM, Wan L, Xiao SG, Xu Y, Weller DK. Directed block copolymer assembly versus electron beam lithography for bit-patterned media with areal density of 1 terabit/inch^2 and beyond. ACS Nano 2009;3:1844–58.
[104] Edwards EW, Montague MF, Solak HH, Hawker CJ, Nealey PF. Precise control over molecular dimensions of block-copolymer domains using the interfacial energy of chemically nanopatterned substrates. Adv Mater 2004;16:1315–9.
[105] Kim SO, Kim BH, Kim K, Koo CM, Stoykovich MP, Nealey PF, Solak HH. Defect structure in thin films of a lamellar block copolymer self-assembled on neutral homogeneous and chemically nanopatterned surfaces. Macromolecules 2006;39:5466–70.
[106] Wang ZG. Response and instabilities of the lamellar phase of diblock copolymers under uniaxial-stress. J Chem Phys 1994;100:2298–309.
[107] Ji SX, Nagpal U, Liu GL, Delcambre SP, Müller M, de Pablo JJ, Nealey PF. Directed assembly of non-equilibrium ABA triblock copolymer morphologies on nanopatterned substrates. ACS Nano 2012;6:5440–8.
[108] Kang H, Detcheverry FA, Mangham AN, Stoykovich MP, Daoulas KC, Hamers RJ, Müller M, de Pablo JJ, Nealey PF. Hierarchical assembly of nanoparticle superstructures from block copolymer–nanoparticle composites. Phys Rev Lett 2008;100:148303/1–148303.
[109] Matsen MW. Elastic properties of a diblock copolymer monolayer and their relevance to bicontinuous microemulsion. J Chem Phys 1999;110:4658–67.
[110] Lipowsky R, Döbereiner HG, Hiergeist C, Indrani V. Membrane curvature induced by polymers and colloids. Physica A: Stat Mech Appl 1998;249:536–43.
[111] Müller M, Gompper G. Elastic properties of polymer interfaces: aggregation of pure diblock, mixed diblock, and triblock copolymers. Phys Rev E: Stat Nonlinear Soft Matter Phys 2002;66:041805/1–41805.
[112] Milner ST. Chain architecture and asymmetry in copolymer microphases. Macromolecules 1994;27:2333–5.
[113] Li RR, Dapkus PD, Thompson ME, Jeong WG, Harrison C, Chaikin PM, Register RA, Adamson DH. Dense arrays of ordered GaAs nanostructures by selective area growth on substrates patterned by block copolymer lithography. Appl Phys Lett 2000;76:1689–91.
[114] Park M, Chaikin PM, Register RA, Adamson DH. Large area dense nanoscale patterning of arbitrary surfaces. Appl Phys Lett 2001;79:257–9.
[115] Asakawa K, Hiraoka T, Hieda H, Sakurai M, Kamata Y. Nanopatterning for patterned media using block copolymer. J Photopolym Sci Technol 2002;15:465–70.
[116] Cheng JY, Ross CA, Thomas EL, Smith HI, Vansco GJ. Fabrication of nanostructures with long-range order using block copolymer lithography. Appl Phys Lett 2002;81:3657–9.
[117] Xu J, Park S, Wang SL, Russell TP, Ocko BM, Checco A. Directed selfassembly of block copolymers on two-dimensional chemical patterns fabricated by electro-oxidation nanolithography. Adv Mater 2010;22:2268–72.
[118] Xu YC, Xie N, Li WH, Qiu F, Shi AC. Phase behaviors and ordering dynamics of diblock copolymer self-assembly directed by lateral hexagonal confinement. J Chem Phys 2012;137:194905/1–194905.
[119] Grason GM, DiDonna BA, Kamien RD. Geometric theory of diblock copolymer phases. Phys Rev Lett 2003;91:058304/1–58304.
[120] Xie N, Li WH, Qiu F, Shi AC. σ phase formed in conformationally asymmetric AB-type block copolymers. ACS Macro Lett 2014;3:906–10.
[121] Tang CB, Lennon EM, Fredrickson GH, Kramer EJ, Hawker CJ. Evolution of block copolymer lithography to highly ordered square arrays. Science 2008;322:429–32.
[122] Ji SX, Nagpal U, Liao W, Liu CC, de Pablo JJ, Nealey PF. Three-dimensional directed assembly of block copolymers together with two-dimensional square and rectangular nanolithograpy. Adv Mater 2011;23:3692–7.
[123] Dessi R, Pinna M, Zvelindovsky AV. Cell dynamics simulations of cylinder-forming diblock copolymers in thin films on topographical and chemically patterned substrates. Macromolecules 2013;46:1923–31.
[124] Chuang VP, Cheng JY, Savas TA, Ross CA. Three-dimensional self-assembly of spherical block copolymer domains into V-shaped grooves. Nano Lett 2006;6:2332–7.
[125] Tang CB, Bang J, Stein GE, Fredrickson GH, Hawker CJ, Kramer EJ, Sprung M, Wang J. Square packing and structural arrangement of ABC triblock copolymer spheres in thin films. Macromolecules 2008;41:4328–39.
[126] Stein GE, Kramer EJ, Li XF, Wang J. Layering transitions in thin films of spherical-domain block copolymers. Macromolecules 2007;40:2453–60.
[127] Chuang VP, Gwyther J, Mickiewicz RA, Manners I, Ross CA. Templated self-assembly of square symmetry arrays from an ABC triblock terpolymer. Nano Lett 2009;9:4364–9.

Please cite this article in press as: Li W, Müller M. Directed self-assembly of block copolymers by chemical or topographical guiding patterns: Optimizing molecular architecture, thin-film properties, and kinetics. Prog Polym Sci (2015), http://dx.doi.org/10.1016/j.progpolymsci.2015.10.008

[128] Son JG, Gwyther J, Chang JB, Berggren KK, Manners I, Ross CA. Highly ordered square arrays from a templated ABC triblock terpolymer. Nano Lett 2011;11:2849–55.
[129] Lee WB, Elliott R, Mezzenga R, Fredrickson GH. Novel phase morphologies in a microphase-separated dendritic polymer melt. Macromolecules 2009;42:849–59.
[130] Nagata Y, Masuda J, Noro A, Cho DY, Takano A, Matsushita Y. Preparation and characterization of a styrene-isoprene undecablock copolymer and its hierarchical microdomain structure in bulk. Macromolecules 2005;38:10220–5.
[131] Matsushita Y. Creation of hierarchically ordered nanophase structures in block polymers having various competing interactions. Macromolecules 2007;40:771–6.
[132] Matsen MW. Effect of architecture on the phase behavior of AB-type block copolymer melts. Macromolecules 2012;45:2161–5.
[133] Takahashi H, Laachi N, Delaney KT, Hur SM, Weinheimer CJ, Shykind D, Fredrickson GH. Defectivity in laterally confined lamella-forming diblock copolymers: Thermodynamic and kinetic aspects. Macromolecules 2012;45:6253–65.
[134] Cooke DM, Shi AC. Effects of polydispersity on phase behavior of diblock copolymers. Macromolecules 2006;39:6661–71.
[135] Schröder-Turk GE, Fogden A, Hyde ST. Local V/A variations as a measure of structural packing frustration in bicontinuous mesophases, and geometric arguments for an alternating Im3m (I-WP) phase in block copolymers with polydispersity. Eur Phys J B 2007;59:115–26.
[136] Meuler AJ, Ellison CJ, Hillmyer MA, Bates FS. Polydispersity-induced stabilization of the core–shell gyroid. Macromolecules 2008;41:6272–5.
[137] Duchs D, Ganesan V, Fredrickson GH, Schmid F. Fluctuation effects in ternary AB + A + B polymeric emulsions. Macromolecules 2003;36:9237–48.
[138] Tanaka H, Hasegawa H, Hashimoto T. Ordered structure in mixtures of a block copolymer and homopolymers. 1. Solubilization of low molecular weight homopolymers. Macromolecules 1991;24:240–51.
[139] Mayes AM, Russell TP, Satija SK, Majkrzak CF. Homopolymer distributions in ordered block copolymers. Macromolecules 1992;25:6523–31.
[140] Hillmyer MA, Maurer WW, Lodge TP, Bates FS, Almdal K. Model bicontinuous microemusion in ternary homopolymer/block copolymer blends. J Phys Chem B 1999;103:4814–24.
[141] Orso KA, Green PF. Phase behavior of thin film blends of block copolymers and homopolymers: changes in domain dimensions. Macromolecules 1999;32:1087–92.
[142] Schwahn D, Mortensen K, Frielinghaus H, Almdal K, Kielhorn L. Thermal composition fluctuations near the isotropic Lifshitz critical point in ternary mixture of a homopolymer blend and diblock copolymer. J Chem Phys 2000;112:5454–72.
[143] Lee JH, Ruegg ML, Balsara NP, Zhu YQ, Gido SP, Krishnamoorti R, Kim MH. Phase behavior of highly immiscible polymer blends stabilized by a balanced block copolymer surfactant. Macromolecules 2003;36:6537–48.
[144] Müller M, Schmid F. Incorporating fluctuations and dynamics in self-consistent field theories for polymer blends. Adv Polym Sci 2005;185:1–58.
[145] Stoykovich MP, Edwards EW, Solak HH, Nealey PF. Phase behavior of symmetric ternary block copolymer–homopolymer blends in thin films and on chemically patterned surfaces. Phys Rev Lett 2006;97:147802/1–147802.
[146] Dotera T. Tricontinuous cubic structures in ABC/A/C copolymer and homopolymer blends. Phys Rev Lett 2002;89:205502/1–205502.
[147] Hayashida K, Takano A, Arai S, Shinohara Y, Amemiya Y, Matsushita Y. Systematic transitions of tiling patterns formed by ABC star-shaped terpolymers. Macromolecules 2006;39:9402–8.
[148] Matsen MW, Bates FS. Origins of complex self-assembly in block copolymers. Macromolecules 1996;29:7641–4.
[149] Martinez-Veracoechea F, Escobedo FA. Bicontinuous phases in diblock copolymer/homopolymer blends: simulation and self-consistent field theory. Macromolecules 2009;42:1775–84.
[150] Martinez-Veracoechea F, Escobedo FA. The plumber's nightmare phase in diblock copolymer/homopolymer blends, a self-consistent field theory study. Macromolecules 2009;42:9058–62.
[151] Burgaz E, Gido SP. T-junction grain boundaries in block copolymer–homopolymer blends. Macromolecules 2000;33:8739–45.
[152] Ruokolainen J, Mäkinen R, Torkkeli M, Mäkelä T, Serimaa R, ten Brinke G, Ikkala O. Switching supramolecular polymeric materials with multiple length scales. Science 1998;280:557–60.
[153] Daoulas KC, Cavallo A, Shenhar R, Müller M. Phase behaviour of quasi-block copolymers: a DFT-based Monte-Carlo study. Soft Matter 2009;5:4499–509.
[154] Lambooy P, Russell TP, Kellogg GJ, Mayes AM, Gallagher PD, Satija SK. Observed frustration in confined block-copolymers. Phys Rev Lett 1994;72:2899–902.
[155] Pickett GT, Balazs AC. Equilibrium orientation of confined diblock copolymer films. Macromolecules 1997;30:3097–103.
[156] Matsen MW. Thin films of block copolymer. J Chem Phys 1997;106:7781–91.
[157] Huang E, Rockford L, Russell TP, Hawker CJ. Nanodomain control in copolymer thin films. Nature 1998;395:757–8.
[158] Matsen MW. Self-assembly of block copolymers in thin films. Curr Opin Colloid Interface Sci 1998;3:40–7.
[159] Geisinger T, Müller M, Binder K. Symmetric diblock copolymers in thin films. I. Phase stability in self-consistent field calculations and Monte Carlo simulations. J Chem Phys 1999;111:5241–50.
[160] Binder K, Müller M. Monte Carlo simulation of block copolymers. Curr Opin Colloid Interface Sci 2000;5:315–23.
[161] Fasolka MJ, Mayes AM. Block copolymer thin films: physics and applications. Annu Rev Mat Res 2001;31:323–55.
[162] Knoll A, Horvat A, Lyakhova KS, Krausch G, Sevink GJA, Zvelindovsky AV, Magerle R. Phase behavior in thin films of cylinder-forming block copolymers. Phys Rev Lett 2002;89:035501/1–35501.
[163] Green PF, Limary R. Block copolymer thin films: pattern formation and phase behavior. Adv Colloid Interface Sci 2001;94:53–81.
[164] Albert JNL, Thomas III HE. Self-assembly of block copolymer thin films. Mater Today 2010;13:24–33.
[165] Radzilowski LH, Carvalho BL, Thomas EL. Structure of minimum thickness and terraced free-standing films of block copolymers. J Polym Sci, B: Polym Phys 1996;34:3081–93.
[166] Matsen MW. Architectural effect on the surface tension of an ABA triblock copolymer melt. Macromolecules 2010;43:1671–4.
[167] Sevink GJA, Zvelindovsky AV, Fraaije JGEM, Huinink HP. Morphology of symmetric block copolymer in a cylindrical pore. J Chem Phys 2001;115:8226–30.
[168] Yu B, Sun PC, Chen TH, Jin QH, Ding DT, Li BH, Shi AC. Confinement induced novel morphologies of block copolymers. Phys Rev Lett 2006;96:138306/1–138306.
[169] Yu B, Sun PC, Chen TH, Jin QH, Ding DT, Li BH, Shi AC. Self-assembly of diblock copolymers confined in cylindrical nanopores. J Chem Phys 2007;127:114906/1–114906.
[170] Geisinger T, Müller M, Binder K. Symmetric diblock copolymers in thin films. II. Comparison of profiles between self-consistent field calculations and Monte Carlo simulations. J Chem Phys 1999;111:5251–8.
[171] Szamel G, Müller M. Thin films of asymmetric triblock copolymers: a Monte Carlo study. J Chem Phys 2003;118:905–13.
[172] Yin YH, Sun PC, Jiang R, Li BH, Chen TH, Jin QH, Ding DT, Shi AC. Simulated annealing study of asymmetric diblock copolymer thin films. J Chem Phys 2006;124:184708/1–184708.
[173] Detcheverry FA, Pike DQ, Nealey PF, Müller M, de Pablo JJ. Monte Carlo simulation of coarse grain polymeric systems. Phys Rev Lett 2009;102:197801/1–197801.
[174] Huinink HP, Brokken-Zijp JCM, van Dijk MA, Sevink GJA. Asymmetric block copolymers confined in a thin film. J Chem Phys 2000;112:2452–62.
[175] Huinink HP, van Dijk MA, Brokken-Zijp JCM, Sevink GJA. Surface-induced transitions in thin films of asymmetric diblock copolymers. Macromolecules 2001;34:5325–30.
[176] Müller M, Smith GD. Phase separation in binary mixtures containing polymers: a quantitative comparison of single-chain-in-mean-field simulations and computer simulations of the corresponding multichain systems. J Polym Sci, B: Polym Phys 2005;43:934–58.
[177] Daoulas KC, Müller M. Single chain in mean field simulations: quasi-instantaneous field approximation and quantitative comparison with Monte Carlo simulations. J Chem Phys 2006;125:184904/1–184904.
[178] Müller M, de Pablo JJ. Computational approaches for the dynamics of structure formation in self-assembling polymeric materials. Annu Rev Mater Res 2013;43:1–34.
[179] Lyakhova KS, Zvelindovsky AV, Sevink GJA, Fraaije JGEM. Inverse mapping of block copolymer morphologies. J Chem Phys 2003;118:8456–9.
[180] Mansky P, Russell TP, Hawker CJ, May J, Cook DC, Satija SK. Interfacial segregation in disordered block copolymers: effect of tunable surface potentials. Phys Rev Lett 1997;79:237–40.

Please cite this article in press as: Li W, Müller M. Directed self-assembly of block copolymers by chemical or topographical guiding patterns: Optimizing molecular architecture, thin-film properties, and kinetics. Prog Polym Sci (2015), http://dx.doi.org/10.1016/j.progpolymsci.2015.10.008

[181] Peters RD, Yang XM, Kim TK, Sohn BH, Nealey PF. Using self-assembled monolayers exposed to X-rays to control the wetting behavior of thin films of diblock copolymers. Langmuir 2000;16:4625–31.
[182] Seshimo T, Bates CM, Dean LM, Cushen D, Durand WJ, Maher MJ, Ellison CJ, Willson CG. Block copolymer orientation control using top coat surface treatments. J Photopolym Sci Tech 2012;25:125–9.
[183] Yoshida H, Suh HS, Ramirez-Hernandez A, Lee JI, Aida K, Wan L, Ishida Y, Tada Y, Ruiz R, de Pablo J, Nealey PF. Topcoat approaches for directed self-assembly of strongly segregating block copolymer thin films. J Photopolym Sci Technol 2013;26:56–8.
[184] Daoulas KC, Müller M, Stoykovich MP, Park SM, Papakonstantopoulos YJ, de Pablo JJ, Nealey PF, Solak HH. Fabrication of complex three-dimensional nanostructures from self-assembling block copolymer materials on two-dimensional chemically patterned templates with mismatched symmetry. Phys Rev Lett 2006;96:036104/1–36104.
[185] Daoulas KC, Müller M, Stoykovich MP, Papakonstantopoulos YJ, de Pablo JJ, Nealey PF, Park SM, Solak HH. Directed assembly of copolymer materials on patterned substrates: balance of simple symmetries in complex structures. J Polym Sci, B: Polym Phys 2006;44:2589–604.
[186] Khaira GS, Qin J, Garner GP, Xiong SS, Wan L, Ruiz R, Jaeger HM, Nealey PF, de Pablo JJ. Evolutionary optimization of directed self-assembly of triblock copolymers on chemically patterned substrates. ACS Macro Lett 2014;3:747–52.
[187] Kim G, Libera M. Morphological development in solvent-cast polystyrene–polybutadiene–polystyrene (SBS) triblock copolymer thin films. Macromolecules 1998;31:2569–77.
[188] Kim S, Briber RM, Karim A, Jones RL, Kim H. Environment-controlled spin coating to rapidly orient microdomains in thin block copolymer films. Macromolecules 2007;40:4102–5.
[189] Yager KG, Fredin NJ, Zhang XH, Berry BC, Karim A, Jones RL. Evolution of block-copolymer order through a moving thermal zone. Soft Matter 2010;6:92–9.
[190] Paradiso SP, Delaney KT, Garcia-Cervera CJ, Ceniceros HD, Fredrickson GH. Block copolymer self assembly during rapid solvent evaporation: insights into cylinder growth and stability. ACS Macro Lett 2014;3:16–20.
[191] Hur SM, Khaira G, Ramirez-Hernandez A, Müller M, Nealey PF, de Pablo JJ. Coarse-grained simulations of defect annihilation in block copolymer thin film via solvent annealing. ACS Macro Lett 2015;4:11–5.
[192] Joanny JF, Leibler L, Ball R. Is chemical mismatch important in polymer-solutions. J Chem Phys 1984;81:4640–56.
[193] Kim SH, Misner MJ, Xu T, Kimura M, Russell TP. Highly oriented and ordered arrays from block copolymers via solvent evparation. Adv Mater 2004;16:226–9.
[194] Phillip WA, Hillmyer MA, Cussler EL. Cylinder orientation mechanism in block copolymer thin films upon solvent evaporation. Macromolecules 2010;43:7763–70.
[195] Albert JNL, Young WS, Lewis RL, Bogart TD, Smith JR, Epps III TH. Systematic study on the effect of solvent removal rate on the morphology of solvent vapor annealed ABA triblock copolymer thin films. ACS Nano 2012;6:459–66.
[196] Tsige M, Grest GS. Molecular dynamics study of the evaporation process in polymer films. Macromolecules 2004;37:4333–5.
[197] Peter S, Meyer H, Baschnagel J. Molecular dynamics simulations of concentrated polymer solutions in thin film geometry. I. Solvent evaporation near the glass transition. J Chem Phys 2009;131:014902/1–14902.
[198] Welander AM, Kang HM, Stuen KO, Solak HH, Müller M, de Pablo JJ, Nealey PF. Rapid directed assembly of block copolymer films at elevated temperatures. Macromolecules 2008;41:2759–61.
[199] Leibler L. Theory of microphase separation in block copolymers. Macromolecules 1980;13:1602–17.
[200] Fredrickson GH, Helfand E. Fluctuation effects in the theory of microphase separation in block copolymers. J Chem Phys 1987;87:697–705.
[201] Elder KR, Viñals J, Grant M. Ordering dynamics in the two-dimensional stochastic Swift–Hohenberg equation. Phys Rev Lett 1992;68:3024–7.
[202] Harrison CK, Adamson DH, Cheng Z, Sebastian JM, Sethuraman S, Huse DA, Register RA, Chaikin PM. Mechanisms of ordering in striped patterns. Science 2000;290:1558–60.
[203] Boyer D, Viñals J. Grain-boundary motion in layered phases. Phys Rev E: Stat Nonlinear Soft Matter Phys 2001;63:061704/1–61704.
[204] Harrison CK, Cheng Z, Sethuraman S, Huse DA, Chaikin PM. Dynamics of pattern coarsening in a two-dimensional smectic system. Phys Rev E: Stat Nonlinear Soft Matter Phys 2002;66:011706/1–11706.
[205] Harrison CK, Angelescu DE, Trawick M, Cheng Z, Huse DA, Chaikin PM, Vega DA, Sebastian JM, Register RA, Adamson DH. Pattern coarsening in a 2D hexagonal system. Europhys Lett 2004;67:800–6.
[206] Vega DA, Harrison CK, Angelescu DE, Trawick ML, Huse DA, Chaikin PM, Register RA. Ordering mechanisms in two-dimensional sphere-forming block copolymers. Phys Rev E: Stat Nonlinear Soft Matter Phys 2005;71:061803/1–61803.
[207] Müller M, Li WH, Orozco Rey JC, Welling U. Kinetics of directed self-assembly of block copolymers on chemically patterned substrates. J Phys Conf Ser 2015;640:012010/1–12010.
[208] Milner ST, Morse DC. Wetting description of block copolymer thin films. Phys Rev E: Stat Nonlinear Soft Matter Phys 1996;54:3793–810.
[209] Tsori Y, Andelman D. Diblock copolymer ordering induced by patterned surfaces. Europhys Lett 2001;53:722–8.
[210] Liu G, Ramírez-Hernández A, Yoshida H, Nygård K, Satapathy DK, Bunk O, de Pablo JJ, Nealey PF. Morphology of lamellae-forming block copolymer films between two orthogonal chemically nanopatterned striped surfaces. Phys Rev Lett 2012;108:065502/1–65502.
[211] Müller M. Geometry-controlled interface localization–delocalization transition in block copolymers. Phys Rev Lett 2012;109:087801/1–87801.
[212] Müller M, Albano EV, Binder K. Symmetric polymer blend confined into a film with antisymmetric surfaces: interplay between wetting behavior and the phase diagram. Phys Rev E: Stat Nonlinear Soft Matter Phys 2000;62:5281–95.
[213] Müller M, Binder K. Interface localization–delocalization transition in a symmetric polymer blend: a finite-size scaling Monte Carlo study. Phys Rev E: Stat Nonlinear Soft Matter Phys 2001;63:021602/1–21602.
[214] Peach M, Koehler JS. The forces exerted on dislocations and the stress fields produced by them. Phys Rev 1950;80:436–9.
[215] Hur SM, Thapar V, Ramirez-Hernandez A, Khaira GS, Segal-Perez T, Ricon-Delglilio PA, Li WH, Müller M, Nealey PF, de Pablo JJ. Molecular pathways for defect annihilation in directed self-assembly. Proc Natl Acad Sci USA 2015, www.pnas.org/cgi/10.1073/pnas.1508225112.
[216] Hashimoto T, Sakamoto N. Nucleation and anisotropic growth of lamellar microdomains in block copolymers. Macromolecules 1995;28:4779–81.
[217] Hashimoto T, Sakamoto N, Koga T. Nucleation and growth of anisotropic grain in block copolymers near order–disorder transition. Phys Rev E: Stat Nonlinear Soft Matter Phys 1996;54:5832–5.
[218] Wickham RA, Shi AC, Wang ZG. Nucleation of stable cylinders from a metastable lamellar phase in a diblock copolymer melt. J Chem Phys 2003;118:10293–305.
[219] Tan HG, Song QG, Niu XH, Gao WF, Yan DD. Sphere-forming diblock copolymers in slit confinement: a dynamic density functional theory study. J Chem Phys 2009;130:214901/1–214901.
[220] Mishra V, Fredrickson GH, Kramer EJ. SCFT simulations of an order–order transition in thin films of diblock and triblock copolymers. Macromolecules 2011;44:5473–80.
[221] Deng HL, Xie N, Li WH, Qiu F, Shi AC. Perfectly ordered patterns via corner-induced heterogeneous nucleation of self-assembling block copolymers confined in hexagonal potential wells. Macromolecules 2015;48:4174–82.
[222] Sota N, Saijo K, Hasegawa H, Hashimoto T. Directed self-assembly of block copolymers into twin bcc-sphere: phase transition process from aligned hex-cylinder to bcc-sphere induced by a temperature jump between the two equilibrium phases. Macromolecules 2013;46:2298–316.

Please cite this article in press as: Li W, Müller M. Directed self-assembly of block copolymers by chemical or topographical guiding patterns: Optimizing molecular architecture, thin-film properties, and kinetics. Prog Polym Sci (2015), http://dx.doi.org/10.1016/j.progpolymsci.2015.10.008